

---

# STATISTICAL COMBINATION OF UNCERTAINTIES

PART 2

JANUARY, 1980

8007090 361

## LEGAL NOTICE

THIS REPORT WAS PREPARED AS AN ACCOUNT OF WORK SPONSORED BY COMBUSTION ENGINEERING, INC. NEITHER COMBUSTION ENGINEERING NOR ANY PERSON ACTING ON ITS BEHALF:

A. MAKES ANY WARRANTY OR REPRESENTATION, EXPRESS OR IMPLIED INCLUDING THE WARRANTIES OF FITNESS FOR A PARTICULAR PURPOSE OR MERCHANTABILITY, WITH RESPECT TO THE ACCURACY, COMPLETENESS, OR USEFULNESS OF THE INFORMATION CONTAINED IN THIS REPORT, OR THAT THE USE OF ANY INFORMATION, APPARATUS, METHOD, OR PROCESS DISCLOSED IN THIS REPORT MAY NOT INFRINGE PRIVATELY OWNED RIGHTS; OR

B. ASSUMES ANY LIABILITIES WITH RESPECT TO THE USE OF, OR FOR DAMAGES RESULTING FROM THE USE OF, ANY INFORMATION, APPARATUS, METHOD OR PROCESS DISCLOSED IN THIS REPORT.

CEN-124(B)-NP

STATISTICAL COMBINATION OF UNCERTAINTIES METHODOLOGY  
PART 2: COMBINATION OF SYSTEM PARAMETER UNCERTAINTIES  
IN THERMAL MARGIN ANALYSES FOR CALVERT CLIFFS UNITS 1&2

## ABSTRACT

This report describes the methods used to statistically combine system parameter uncertainties in the thermal margin analyses for Calvert Cliffs Units 1 and 2 cores. A detailed description of the uncertainty probability distributions and response surface techniques used is presented. This report demonstrates that there will be at least 95% probability with at least 95% confidence that the limiting fuel pin will avoid departure from nucleate boiling (DNB) so long as the minimum DNB ratio found with the best estimate design TORC model remains above 1.23.



## TABLE OF CONTENTS

<u>Title</u>	<u>Page</u>
Abstract	i.
Table of Contents	ii.
List of Figures	iv.
List of Tables	v.
Nomenclature and Abbreviations	vi.
1.0 Summary of Results	1-1
2.0 Introduction	2-1
2.1 Deterministic Method	2-2
2.2 Statistical Method	2-2
3.0 Sources of Uncertainty	3-1
3.1 State Parameters Used in the Study	3-1
3.1.1 Method for Selecting State Parameters	3-2
3.1.2 Inlet Flow Perturbation Sensitivity	3-3
3.1.3 Enthalpy Rise Factor Sensitivity	3-3
3.1.4 Systematic Pitch Reduction Sensitivity	3-4
3.1.5 Most Adverse State Parameters	3-5
3.2 Radial Power Distribution	3-5
3.3 Inlet Flow Distribution	3-6
3.4 Exit Pressure Distribution	3-6
3.5 Enthalpy Rise Factor	3-7
3.6 Heat Flux Factor	3-7
3.7 Clad O. D.	3-7
3.8 Systematic Pitch Reduction	3-8
3.9 Fuel Rod Bow	3-8

TABLE OF CONTENTS (con't.)

<u>Title</u>	<u>Page</u>
3.10 CHF Correlation	3-8
3.11 TORC Code Uncertainty	3-9
4.0 MDNBR Response Surface	4-1
4.1 TORC Model Used	4-1
4.2 Variables Used	4-1
4.3 Experiment Design	4-2
4.4 Design Matrix	4-3
4.5 Response Surface	4-3
5.0 Combination of Probability Distribution Functions	5-1
5.1 Method	5-1
5.2 Results	5-2
5.3 Analytical Comparison	5-2
6.0 Application to Design Analysis	6-1
6.1 Statistically Derived MDNBR Limit	6-1
6.2 Adjustments to Statistically Derived MDNBR Limit	6-1
6.3 Application to TORC Design Model	6-2
7.0 Conclusions	7-1
7.1 Conservatism in the Methodology	7-1
8.0 References	8-1
Appendix	
Appendix A: Detailed TORC Analyses Used to Generate Response Surface	A-1

## LIST OF FIGURES

<u>Fig. No.</u>	<u>Title</u>	<u>Page</u>
3-1	Inlet Flow Distribution Used to Establish State Parameters for Response Surface	3-10
3-2	Exit Pressure Distribution Used to Establish State Parameters for Response Surface	3-11
3-3	Core Wide Radial Power Distribution Used to Establish State Parameters for Response Surface	3-12
3-4	Hot Assembly Radial Power Distribution Used to Establish State Parameters for Response Surface	3-13
3-5	Channel Numbering Scheme for Stage 1 TORC Analysis to Establish Response Surface State Parameters	3-14
3-6	Channel Numbering Scheme for Stage 2 TORC Analysis to Establish Response Surface State Parameters	3-15
3-7	Third Stage Channel and Fuel Pin Numbering Schemes Used in TORC Analysis to Establish Response Surface State Parameters	3-16
3-8	Inlet Flow Factors for Seized Rotor Analysis of 217 Bundle 14x14 Assembly Cores	3-17
3-9	Exit Pressure Distribution Used in Sensitivity Study	3-18
4-1	Core Wide Power Distribution Used to Generate Response Surface	4-5
4-2	Hot Assembly Radial Power Distribution Used to Generate Response Surface	4-6
4-3	Intermediate (2nd Stage) TORC Model Used in Generating Response Surface	4-7
4-4	Subchannel (3rd Stage) TORC Model Used in Generating Response Surface	4-8
5-1	Resultant MDNBR Probability Distribution Function	5-5

## LIST OF TABLES

<u>Table No.</u>	<u>Title</u>	<u>Page</u>
3-1	Ranges of Operating Conditions for Which Response Surface Is Valid	3-19
3-2	Nominal and Perturbed Flow for Establishing Sensitivity of Flow Distribution Effects on MDNBR to Operating Conditions	3-20
3-3	Flow Perturbation Effects at Various Operating Conditions	3-21
3-4	Sensitivity of Enthalpy Rise Factor Effects to Axial Shape Index (Isolated Hot Assembly Model)	3-22
3-5	Sensitivity of Enthalpy Rise Factor Effects to Operating Conditions (Isolated Hot Assembly Model)	3-23
3-6	Sensitivity of Enthalpy Rise Factor Effects to Axial Shape Index (Core Wide Analysis)	3-24
3-7	Sensitivity of Systematic Pitch Reduction Effects to Operating Conditions	3-25
3-8	State Parameters Which Maximize Sensitivity of MDNBR to System Parameters	3-26
3-9	Sensitivity of MDNBR to Inlet Flow Distribution	3-27
3-10	Sensitivity of MDNBR to Exit Pressure Distribution	3-28
3-11	As-Built Clad O.D. (inches) Data for 14x14 Fuel	3-29
3-12	As-Built Gap Width Data (inches)	3-30
4-1	State Parameters Included as Variables in the Response Surface	4-9
4-2	Coefficients for MDNBR Response Surface	4-10
5-1	Probability Distribution Functions Combined by SIGMA	5-4
A-1	Coded Set of Detailed TORC Cases Used to Generate Response Surface	A-2
A-2	Comparison of TORC and Response Surface MDNBR for Cases Used to Generate Response Surface	A-13

## NOMENCLATURE AND ABBREVIATIONS

b	coefficient in response surface
c	constant in response surface
f	arbitrary functional relationship
k	number of independent variables in response surface
n	number of items in a sample
p.d.f.	probability distribution function
psf	pounds per square foot
psia	pounds per square inch (absolute)
x	system parameter
y	state parameter
z	MDNBR values predicted by response surface
ASI	axial shape index (defined in Table 3-3)
CE	Combustion Engineering
CHF	Critical Heat Flux
DNB	Departure from Nucleate Boiling
DNBR	Departure from Nucleate Boiling Ratio
F	Fahrenheit
$F_q''$	engineering heat flux factor
MDNBR	Minimum Departure from Nucleate Boiling
T	temperature
T-H	thermal-hydraulic
$\alpha$	constant used to code system parameters (Table 4-1)
$\epsilon$	constant used to code system parameters (Table 4-1)
$\eta$	coded value of system parameters (Table 4-1)
$\mu$	mean
$\sigma$	standard deviation
$\Delta$	denotes difference between two parameters

subscripts

- denotes vector quantity
- i index
- in conditions at reactor core inlet
- j index

superscripts

- ^ denotes estimate
- 0 degrees
- average value

## 1.0 Summary of Results

Methods were developed to combine statistically the uncertainties in reference thermal margin (Detailed TORC) analyses. These methods were applied to the Calvert Cliffs I, and Calvert Cliffs II cores. This work demonstrated that there will be at least 95% probability with at least 95% confidence that the limiting fuel pin will avoid departure from nucleate boiling (DNB) so long as the Minimum DNB Ratio (MDNBR) found with the best estimate design TORC model remains above 1.23. The 1.23 MDNBR limit includes allowances for reference analysis input uncertainties but does not take into account uncertainties in operating conditions (e.g. monitoring uncertainties). An improved treatment of operating condition uncertainties has been developed in Part 1 of this report (1-1).

## 2.0 Introduction

C-E's thermal margin methodology for Calvert Cliffs I and II has been modified by the application of statistical methods. This part of the report focuses on the statistical combination of reference thermal-hydraulic (T-H) code input uncertainties. This combination was accomplished by the generation of a Minimum DNBR (MBNBR) response surface and the application of Monte Carlo methods.

A complete description of the methods used in the statistical combination is provided in this report. The remainder of this section outlines the previous deterministic and the new statistical thermal margin methods. Section 3.0 describes the sources of uncertainty that were considered in this effort. Section 4.0 describes the MDNBR response surface. The application of Monte Carlo Methods is discussed in Section 5.0, and results are presented. Finally Section 6.0 describes the changes in design analyses that result from this work.



## 2.1 Deterministic Method

Two types of problem dependent data are required before a detailed T-H code can be applied. The first type of data, system parameters, describe the physical system under consideration and are not monitored with the detail needed for detailed T-H analysis while the reactor is operational. System parameters describe the reactor geometry, pin by pin radial power distributions, inlet and exit flow boundary condition, etc. The second type of data, state parameters, describe the operational state of the reactor. State parameters are monitored while the reactor is in operation and include the core average inlet temperature, primary loop flow rate, primary loop pressure, etc.

C-E thermal margin methods (2-1) utilize the TORC code (2-2) and the CE-1 CHF correlation (2-3) with two types of models. The first model, detailed TORC, is tailored to yield best estimate MDNBR predictions in a particular fuel assembly for a specific power distribution. Both system and state parameter input are used in a detailed TORC model. The second model, design TORC, requires only state parameter data and may be applied to any fuel assembly for any power distribution that is expected to occur during a particular fuel cycle. System parameters are fixed in the design model so that the model will yield either accurate or conservative MDNBR predictions for all operating conditions within a specified range.

Design model MDNBR results are verified by comparison with results from the detailed model of the limiting assembly in the deterministic method. After the design model is shown to yield acceptable (i.e. accurate or conservative) results, additional adjustment factors are applied to account for uncertainties in system parameter input to the detailed model. For example, engineering factors are applied to the hot subchannel of the design model to account for fuel fabrication uncertainties. These adjustment factors, though arrived at statistically, are applied in a deterministic manner. That is, although each adjustment factor represents a 95/95 probability/confidence limit that the particular parameter deviation from nominal is no worse than described by that factor, all factors are applied simultaneously to the limiting subchannel. This is equivalent to assuming that all adverse deviations occur simultaneously in the limiting subchannel.

## 2.2 Statistical Method

The probability of all adverse system parameter deviations from nominal occurring simultaneously in the limiting subchannel is extremely remote. With a more reasonable, demonstrably conservative method, the probability of system parameter input being more adverse than specified can be taken into account statistically, as described herein.

The improved methodology involves a statistical combination of system parameter uncertainties with the CHF correlation uncertainties to determine

a revised design MDNBR limit. Since uncertainties in system parameters are taken into account in the derivation of the new MDNBR limit, no other allowance need be made for them. A best estimate design TORC model is therefore used with the revised MDNBR limit for thermal margin analysis. This best estimate design model yields conservative or accurate MDNBR results when compared with a best estimate detailed model. An increased MDNBR limit is then applied to the design model to account for system parameter uncertainties. The resultant best estimate design model and increased MDNBR limit ensure with at least 95% probability and at least a 95% confidence level that the limiting fuel pin will avoid a departure from nucleate boiling if the predicted MDNBR is not below the limit MDNBR.

### 3.0 Sources of Uncertainty

Four types of uncertainty are identified in MDNBR predictions from the TORC code:

- i) numerical solution parameter uncertainty
- ii) code uncertainty
- iii) state parameter uncertainty
- iv) system parameter uncertainty

Numerical solution parameters are required input that would not be necessary if analytic methods could be used (e.g. radial mesh size, axial mesh size, convergence criteria, etc.). The uncertainties associated with these parameters are dealt with in a conservative manner(3-1) in C-E's present methodology.

The numerical algorithms in the TORC code represent approximations to the conservation equations of mass, momentum, and energy. Because of the approximations involved, an inherent code uncertainty exists. This uncertainty is implicitly dealt with in the CE-1 CHF correlation (3-3) (3-4).

State parameters, as explained in section 2.1, define the operational state of the reactor. The treatment of uncertainties in these parameters is addressed in reference 3-2 .

As explained in section 2.1, system parameters describe the physical environment that the working fluid encounters. This report establishes the equivalent MDNBR uncertainty that results from a statistical combination of uncertainties in system parameters.

#### 3.1 State Parameters Used in the Study

Generation of a response surface which simultaneously relates MDNBR to both system and state parameters would require an excessive number of detailed TORC analyses. Consequently a conservative approximation is made and a response surface relating MDNBR to system parameters only is created. To achieve conservatism, it is necessary to generate the surface for that set of state parameters which maximizes the sensitivity of MDNBR to system parameter variations. That is, the response surface can be described as:

$$\text{MDNBR} = g(\underline{x}, \underline{y}_0)$$

where  $\underline{y}_0$ , the vector of state parameters, is selected such that

$$\left| \frac{\partial(\text{MDNBR})}{\partial \underline{x}} \right|_{\underline{y}_0} \rightarrow \text{maximum}$$

The set of state parameters,  $y_0$ , that satisfies the above relation, is referred to as the most adverse set of state parameters. The generation of the response surface is discussed in section 4.3.

### 3.1.1 Method for Selecting State Parameters

Allowable operating parameter ranges are presented in Table 3-1. These ranges are based upon reactor setpoints including measurement uncertainty. The response surface must be valid over these ranges. As indicated above, a single set of operating conditions is chosen from these ranges to maximize the sensitivity of MDNBR to system parameters.

This set of state conditions is determined from detailed TORC analyses in the following manner. Two TORC analyses are performed for a single set of operating conditions. In the first analysis, nominal system parameters are used and the core average heat flux is chosen to yield a MDNBR in the neighborhood of 1.19. The second TORC analysis uses the same heat flux and operating conditions but has one of the system parameters perturbed. The MDNBR from the "perturbed" analysis is then subtracted from the "nominal" MDNBR to yield a  $\Delta$ MDNBR for the chosen set of operating conditions. That is

$$\Delta\text{MDNBR} = \text{"Nominal" MDNBR} - \text{"Perturbed" MDNBR} \quad (3.1)$$

The percent change in MDNBR is then determined according to the relation:

$$\% \text{Change} = (\Delta\text{MDNBR} / \text{"Nominal" MDNBR}) \times 100 \quad (3.2)$$

This process is repeated for several sets of operating conditions to establish the sensitivity of the  $\Delta$ MDNBR throughout the allowable operating range. Sets of operating conditions used in this sensitivity study are chosen to envelop the required ranges shown in Table 3-1. The operating conditions which yield the maximum percent change in MDNBR are those which maximize the sensitivity of the MDNBR to the perturbed system parameter. These state parameters are referred to as the "most adverse" state parameters.

Since MDNBR is a smoothly varying function of these parameters (3-3), it is likely that the theoretical most adverse state parameters will be similar to the most adverse set found by the method described above. Similarly, it is also highly unlikely that MDNBR sensitivities observed with the theoretical most adverse set will differ appreciably from MDNBR sensitivities which occur using the most adverse set found by the above method.

The detailed TORC model used in these cases is for one of the limiting assembly candidates of the Calvert Cliffs Unit 1, Cycle 3 core. In this model core geometry is identical, and boundary conditions are similar to the Calvert Cliffs Unit I and Calvert Cliffs Unit II

cores. Hence, trends in the sensitivity of MDNBR to variations in system parameters at various operating conditions will be the same for all of these cores. The radial power distribution used in the sensitivity study differs from the distribution used to generate the response surface. The sensitivity of MDNBR to state parameters will exhibit the same trends regardless of radial power distribution since the local coolant conditions in the hot assembly will be similar at 1.19 MDNBR. Hence, the most adverse set of state parameters found in this study may be applied to generate the response surface.

Inlet flow and exit pressure boundary conditions for the model are shown in Fig. 3-1 and 3-2. Core-wide and hot assembly power distributions are shown in Fig. 3-3 and 3-4 respectively. The detailed TORC analysis (3-1) consists of three stages. A core-wide analysis is done in the first stage, in which each fuel assembly near the limiting assembly is modeled as an individual channel. Crossflow boundary conditions from the first stage are applied in the second stage to a more detailed model of the neighborhood around the limiting assembly. Each quadrant of the limiting assembly is represented by a channel in the second stage analysis. Crossflow boundary conditions from the second stage are applied to the subchannel model of the limiting assembly hot quadrant in the third stage, and the MDNBR is calculated. TORC models for the first, second, and third stages of the model used in the sensitivity study are shown in Fig. 3-5, 3-6, and 3-7 respectively.

### 3.1.2 Inlet Flow Perturbation Sensitivity

As indicated in Fig. 3-3, the hot assembly occurs in channel 9 of the first stage TORC model. A perturbed model for use in determining the sensitivity of inlet flow distribution effects on MDNBR to operating conditions is created by reducing the inlet flow fraction to the hot assembly and an adjacent assembly. Inlet flow is also increased accordingly in two assemblies far from the hot assembly to preserve continuity. Inlet flow fractions for the perturbed and nominal models are presented in Table 3-2.

The sensitivity of flow distribution effects on MDNBR to operating conditions found with the above models is presented in Table 3-3. MDNBR is most sensitive to variations in the inlet flow distribution for an axial shape index of [ ]. Greatest sensitivity to flow perturbations is observed with a pressure/temperature/flow combination of [ ]. Hence the greatest sensitivity is expected to occur for the operating conditions:

[ ]

### 3.1.3 Enthalpy Rise Factor Sensitivity

The method described in section 3.1.1 is altered slightly to determine the state parameters which maximize MDNBR sensitivity to the enthalpy



rise factor. The uncertainties accommodated by the enthalpy rise factor are discussed in Reference (3-4). Since the enthalpy rise factor affects only the limiting subchannel and adjacent subchannels, an isolated model of the limiting assembly hot quadrant is used to reduce computational time. The isolated quadrant model is simply the hot quadrant subchannel model shown in Fig. 3-7 with adiabatic, impervious boundary conditions imposed on the sides of the quadrant. Observed trends in behavior found with TORC analyses of the isolated quadrant model are confirmed by multistage TORC analyses. Nominal cases are run with no enthalpy rise factor. An enthalpy rise factor of 1.03 is applied to the fuel pins which bound the limiting subchannel in the perturbed cases.

Results found with the isolated TORC model are shown in Tables 3-4 and 3-5. The data in these tables indicate that MDNBR sensitivity to the enthalpy rise factor is maximized with [ ] axial shape indices, corresponding to [ ] power distributions, and the pressure/temperature/flow combination [ ]

Data from multistage TORC analyses are presented in Table 3-6. These data show a similar trend when compared with the isolated quadrant model data of Table 3-4, however maximum sensitivity is seen at a [ ] axial shape index. The greatest sensitivity of MDNBR to the enthalpy rise factor is expected to occur for the operating conditions:

[ ]

#### 3.1.4 Systematic Pitch Reduction Sensitivity

Systematic pitch reduction uniformly decreases fuel rod pitch throughout an entire fuel assembly. Nominal pitch for 14 x 14 C-E fuel is 0.58". Hot assembly fuel pitch is reduced to [ ] in the limiting assembly of the perturbed model used to establish the sensitivity of systematic pitch reduction effects on MDNBR to operating conditions.

Results from nominal and perturbed pitch TORC analyses are shown in Table 3-7. Based upon these data, maximum MDNBR sensitivity to systematic pitch reduction is expected to occur at:

[ ]

Data in Table 3-7 also indicate that the sensitivity of MDNBR to systematic pitch [ ]

### 3.1.5 Most Adverse State Parameters

As explained in section 3.1.0, the set of state parameters chosen for use in generating the response surface should maximize MDNBR sensitivity to variations in system parameters; this is the most adverse set of state parameters. The most adverse set of parameters is chosen for use in generating the response surface so that the resultant MDNBR uncertainty will be maximized. This introduces conservatism into the overall treatment.

The state parameters which maximize MDNBR sensitivity to various system parameters are listed in Table 3-8. This comparison indicates that [ ]psia and [ ]design flow are respectively the most adverse system pressure and flow rates. The most adverse axial shape index (A.S.I.) and inlet temperature ( $T_{in}$ ) are not evident from this comparison. The magnitude and impact of each system parameter uncertainty must also be considered in choosing the most adverse values of A.S.I. and  $T_{in}$ .

Magnitudes of each of the system parameter uncertainties are assigned and discussed in Sections 3.2 - 3.8. The magnitude and impact of the [ ] those of the other system parameters. Therefore, the A.S.I. and  $T_{in}$  which tend to maximize MDNBR sensitivity to the [ ] are used to generate the response surface. Although maximum MDNBR sensitivity to [ ] is observed with [ ] A.S.I., this sensitivity is only slightly less than the sensitivity observed with a [ ] A.S.I., as shown by the data in Table 3-3. Since sensitivity to enthalpy rise factor increases with [ ] A.S.I., [ ] is selected as most adverse. The most adverse set of state parameters is thus:

$$\left[ \begin{array}{l} \text{ } \\ \text{ } \\ \text{ } \end{array} \right]$$

where 100% design flow is 370,000 gpm.

### 3.2 Radial Power Distribution

The PDQ computer code (3-5) is used to predict planar radial power distributions throughout the life of a core for enveloping operating conditions. Limiting power distributions are selected from the above set and are used as input to TORC DNB analyses. Comparisons between PDQ predictions and measured data (3-6) show that PDQ overpredicts radial peaking factors in the peripheral regions of the reactor (i.e. the outermost three rows of fuel assemblies).

Inlet flow distributions for four-loop operation and seized rotor accident analysis of CE's 14 x 14 cores are shown in Fig. 3-1 and 3-8 respectively. These distributions manifest the following trend: the central portion of the core receives higher than average

inlet flow while the peripheral assemblies receive lower than average inlet flow. For this reason, the limiting assembly for DNB analysis is found on the core periphery.

Since the PDQ power distributions overpredict power in the peripheral assemblies, and the limiting assembly for DNB analysis is among these assemblies, the use of PDQ data in DNB analyses is conservative. This inherent conservatism in the thermal margin methodology makes it unnecessary to account for uncertainties in the radial power distributions that are used in TORC DNB analyses.

### 3.3 Inlet Flow Distribution

An inlet flow boundary condition is used in detailed TORC analysis. Ratios of the local to core average mass velocity are input for every flow channel in the core-wide analysis. Mean values of the inlet flow splits for three pump operation are presented in Fig. 3-8. A large part of the uncertainty in the flow splits results from measurement uncertainty. This measurement uncertainty is considered random and may be characterized by a normal probability distribution function (p.d.f.).

A sensitivity study, conducted to determine the effects of inlet flow variations in assemblies which neighbor the limiting assembly, yields the results presented in Table 3-9. Channel numbers in this table refer to Fig. 3-5. Flow in the assemblies diagonally adjacent to the limiting assembly is decreased by 3, 6, and 9 percent for bottom peaked axial power profiles and by 9 percent for a top peaked profile. These perturbations are in excess of inlet flow uncertainties, yet only minor changes in MDNBR are observed.

The above sensitivity study has shown that MDNBR in the limiting assembly is unaffected by changes in the inlet flow of assemblies which are diagonally adjacent to the limiting assembly. Because of this insensitivity, inlet flow in assemblies which are diagonally adjacent to the limiting assembly may be omitted from the response surface. Only inlet flow to the limiting assembly and those assemblies which are immediately adjacent to it are included in the response surface.

### 3.4 Exit Pressure Distribution

Sensitivity studies conducted to establish the impact on MDNBR of variations in the exit pressure distribution are summarized in Table 3-10. Detailed TORC analyses are performed with nominal and extreme exit pressure distributions, as shown in Fig. 3-9. The exit pressure in the limiting assembly is increased to the 95% probability level while the exit pressures in the assemblies adjacent to the limiting assembly are also increased to yield an approximate 95% probability level for the three adjacent assembly exit pressures in the extreme exit pressure distribution. Channel 4 of Fig. 3-5 is the limiting channel in this study. Detailed TORC analyses performed with both bottom peaked and top peaked axial power profiles demonstrate that MDNBR is extremely insensitive to variations in the exit pressure distribution. Consequently, the exit pressure distribution need not be included in the MDNBR response surface.



### 3.5 Enthalpy Rise Factor

The engineering enthalpy rise factor accounts for the effects of manufacturing deviations in fuel fabrication from nominal dimensions and specifications on the enthalpy rise in the subchannel adjacent to the rod with the MDNBR. Tolerance deviations in fuel pellet density, enrichment, and diameter averaged over the length of the fuel rods are used to compute this factor.

A survey of as-built data for 14x14 fuel indicates that the enthalpy rise factor may be characterized by a normal distribution with a mean of 1.0 and standard deviation of 0.010. Since these values are determined using data for every rod in the core, there is >95% confidence that the population mean and standard deviation are no larger than these values. Applicability of these data to future reload cycles will be verified.

### 3.6 Heat Flux Factor

The engineering heat flux factor is used to take into account the effect on local heat flux of deviations from nominal design and specifications that occur in fabrication of the fuel. Random variation in pellet enrichment, initial pellet density, pellet diameter, and clad outside diameter contribute to the effects represented by the engineering heat flux factor. Tolerance limits and fuel specifications ensure that this factor may be characterized conservatively by a normal p.d.f. with a mean of 1.0 and standard deviation of 0.015. Since these values are based upon tolerance limits, there is >95% confidence that the population mean and standard deviation are no larger than these values.

### 3.7 Clad O.D.

Variations in clad diameter change subchannel flow area and also change the local heat flux. The impact of both random and systematic variations in fuel clad O.D. on the local heat flux is accounted for by the engineering factor on heat flux, discussed in section 3.6. The effect of random variations in clad O.D. on subchannel flow area is included in the rod bow penalty, discussed in section 3.9. The effect of systematic variations in clad O.D. on the subchannel hydraulic parameters is addressed here.

Manufacturing tolerances on the fuel clad allow for the possibility that the clad diameter will be systematically above nominal throughout an entire fuel assembly. That is to say, the mean as-built value of the clad O.D. may differ from the nominal value. The distribution of the mean clad O.D. for fuel assemblies may be characterized by a normal p.d.f. with a mean equal to the mean clad O.D. and a standard deviation given by the relation (3-7) :

$$\sigma_{\bar{A}} = \sigma \sqrt{\frac{(N-n)}{n(N-1)}} \quad (3.3)$$

where N is the number of specimens in the parent population and n is the sample size.

As built data for C-E's 14 x 14 fuel are presented in Table 3-11. The minimum systematic clad O.D. is [ ] while the maximum systematic clad O.D. is [ ]. Since the adverse effect of clad O.D. variations is already taken into account by the engineering heat flux factor, and use of a less than nominal clad O. D. would increase subchannel flow area, benefitting the MDNBR, the maximum value [ ] is used in this study. The standard deviation of the mean at the 95% confidence limit is [ ] in. The double accounting for both the adverse effect of a decrease in clad O.D. in the engineering factor on heat flux and the adverse effect of a systematic increase in clad O.D. on subchannel flow area adds conservatism to the analysis.

### 3.8 Systematic Pitch Reduction

The rod bow penalty, discussed in section 3.9, takes into account the adverse effect on MDNBR that results from random variations in fuel rod pitch. The rod bow penalty does not take into account the adverse effect of systematic variations in fuel rod pitch. This systematic pitch reduction effect must be discussed separately.

Manufacturing tolerances on fuel assemblies allow for the possibility that the as-built fuel pitch will be less than nominal throughout an entire fuel assembly. Thus the systematic pitch refers to the mean value of the pitch in an assembly. The systematic pitch distribution is assumed to be a normal distribution characterized by the mean value of the pitch and the standard deviation of that mean value.

As-built gap width data for C-E's 14 x 14 fuel are presented in Table 3-12. The minimum systematic gap width is seen to occur in the Calvert Cliffs 1 [ ] and is [ ] inches. This, combined with the maximum clad O.D. from section 3.7 indicates that the minimum pitch is [ ]. At the 95% confidence level, the standard deviation of the mean is [ ] inches.

### 3.9 Fuel Rod Bow

The fuel rod bow penalty accounts for the adverse impact on MDNBR of random variations in spacing between fuel rods. The methodology for determining the rod bow penalty is the subject of a C-E topical report (3-8). Appendix G of that report (3-9) applies a formula derived by the NRC (3-10) to compute the rod bow penalty for C-E fuel. The penalty at 45,000 MWd/MTU for CE's 14 x 14 fuel is 0.6% in DNBR. This penalty is applied directly to the new MDNBR limit derived in Section 5.

### 3.10 CHF Correlation

The C-E 1 Critical Heat Flux (CHF) correlation (3-11) (3-12) is used in the TORC code (3-1) to determine whether a departure from nucleate boiling (DNB) will occur. This correlation is based on a set of 731

data points. The mean of the ratio of observed to predicted CHF using the CE-1 correlation is 0.99983, while the standard deviation of that ratio is 0.06757. CHF correlation uncertainty may be characterized by a normal distribution with a mean of 0.99983 and standard deviation of 0.06757. This yields a 1.13 MDNBR limit to satisfy the criterion of "95% probability at the 95% confidence level that the limiting fuel pin does not experience DNB". However, because the NRC staff has not yet concluded its review of the CE-1 correlation, a 5% penalty has been applied; this raises the 95/95 DNBR limit to 1.19. This penalty may be conservatively treated by assuming a displaced Gaussian distribution with a mean of 1.06 and the same standard deviation as above.

### 3.11 TORC Code Uncertainty

The TORC computer code (3-1) represents an approximate solution to the conservation equations of mass, momentum, and energy. Simplifying assumptions were made, and experimental correlations were used to arrive at the algorithms contained in the TORC code. Hence, the code has associated with it an inherent calculational uncertainty. Comparisons between TORC predictions and experimental data (3-10)(3-13) have shown that TORC is capable of adequate predictions of coolant conditions.

As explained in Section 5.0 of Reference (3-13), the TORC code was used to determine local coolant conditions from data obtained during the CE-1 CHF experiments. These local coolant conditions were then used to develop the CE-1 CHF correlation. Thus, any calculational uncertainty in the TORC code is implicitly included in the MDNBR limit that is used with the TORC/CE-1 package in thermal margin analyses.

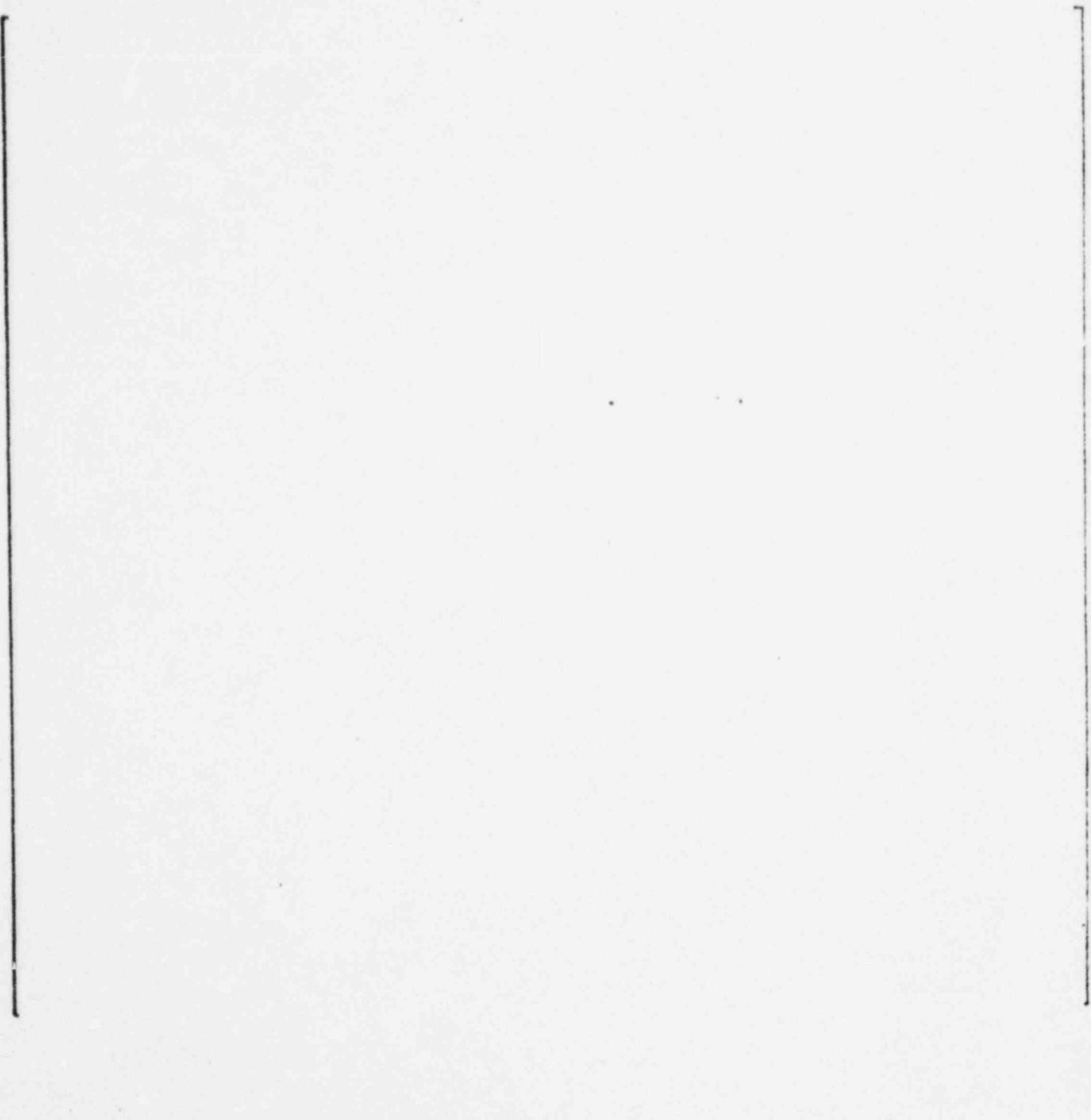


FIGURE 3-1  
INLET FLOW DISTRIBUTION USED TO ESTABLISH STATE PARAMETERS  
FOR RESPONSE SURFACE


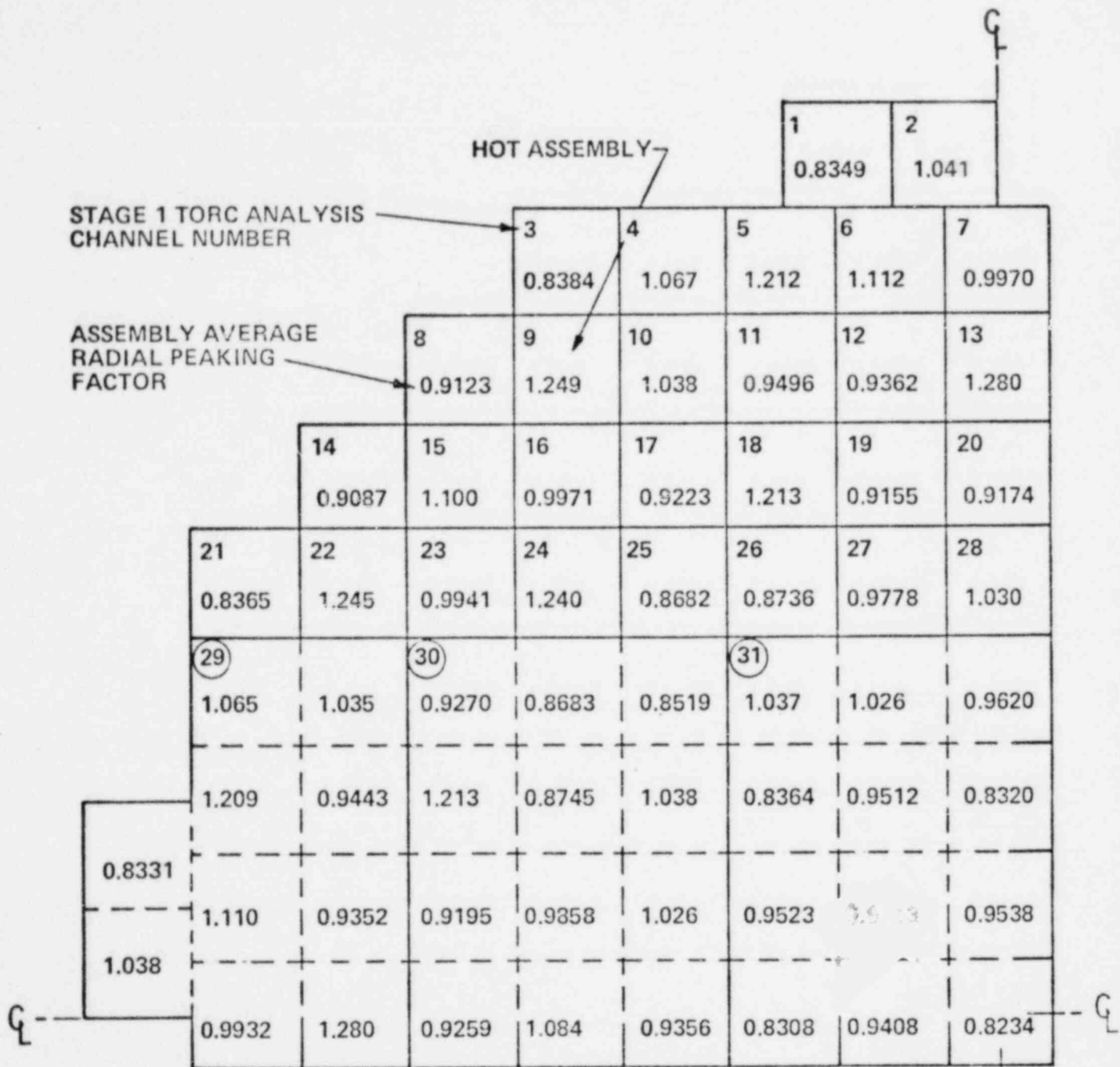


FIGURE 3-2  
EXIT PRESSURE DISTRIBUTION USED TO ESTABLISH STATE PARAMETERS  
FOR RESPONSE SURFACE



Note: Circled channel numbers denote flow channels in which several fuel assemblies have been "lumped" into a single channel for T-H analysis.

FIGURE 3-3  
CORE WIDE RADIAL POWER DISTRIBUTION USED TO ESTABLISH STATE  
PARAMETERS FOR RESPONSE SURFACE

denotes assembly quadrant average radial peaking factor

		$F_R = 1.185$								$F_R = 1.303$			
						LOCATION 9							
1.174	1.189	1.214	1.243	1.286	1.374								
1.210	1.231	1.261	1.282	1.297	1.335	1.338							
1.256	1.298	1.359	1.370	1.333	1.310	1.313							
1.299	1.371	$F_R = 1.314$		1.384	1.309	1.284				$F_R = 1.332$			
1.319	1.389			1.387	1.304	1.272							
1.321	1.358	1.409	1.406	1.347	1.293	1.269							
1.341	1.357	1.373	1.365	1.335	1.305	1.287							

FIGURE 3-4  
HOT ASSEMBLY RADIAL POWER DISTRIBUTION USED TO ESTABLISH  
STATE PARAMETERS FOR RESPONSE SURFACE





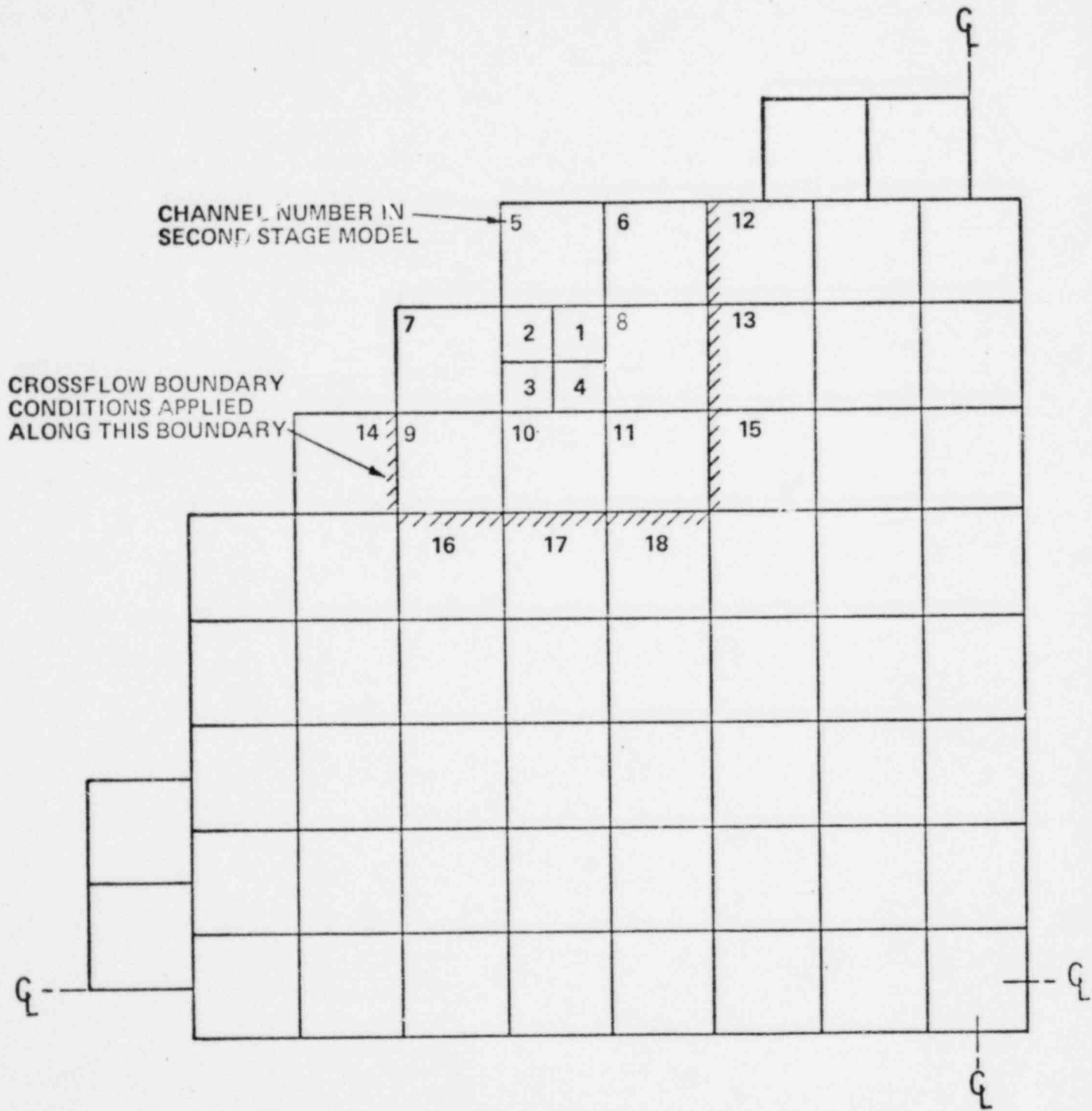


FIGURE 3-6  
 CHANNEL NUMBERING SCHEME FOR STAGE 2 TORC ANALYSIS  
 TO ESTABLISH RESPONSE SURFACE STATE PARAMETERS

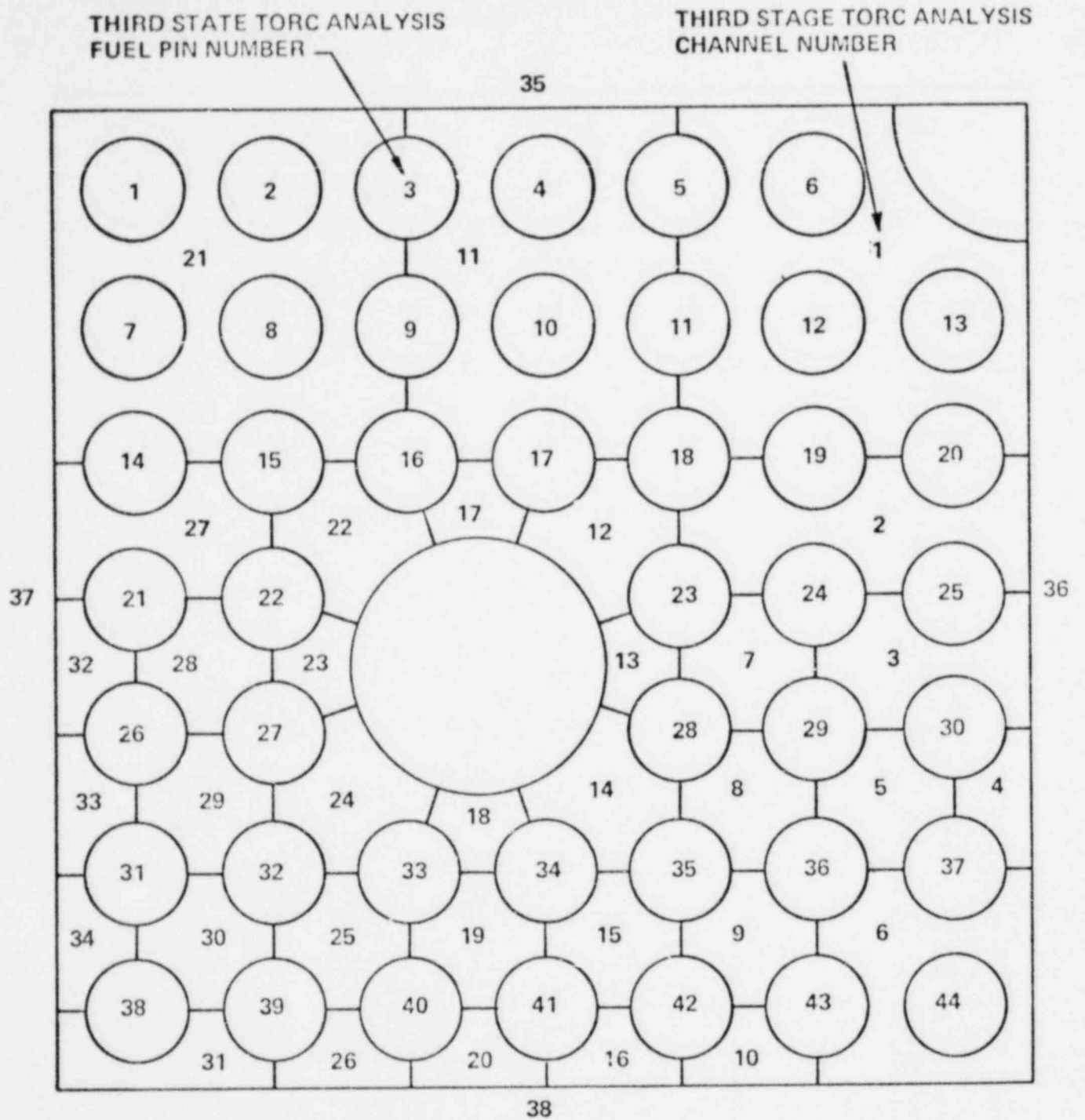


FIGURE 3-7  
 THIRD STAGE CHANNEL AND FUEL PIN NUMBERING SCHEME USED IN TORC  
 ANALYSES TO ESTABLISH RESPONSE SURFACE STATE PARAMETERS

FIGURE 3-8  
INLET FLOW FACTORS FOR SEIZED ROTOR ANALYSIS OF 217 BUNDLE  
14x14 ASSEMBLY CORES

VALUES DENOTE DEVIATION OF ASSEMBLY AVERAGE  
EXIT PRESSURE FROM CORE AVERAGE EXIT PRESSURE (PSF)

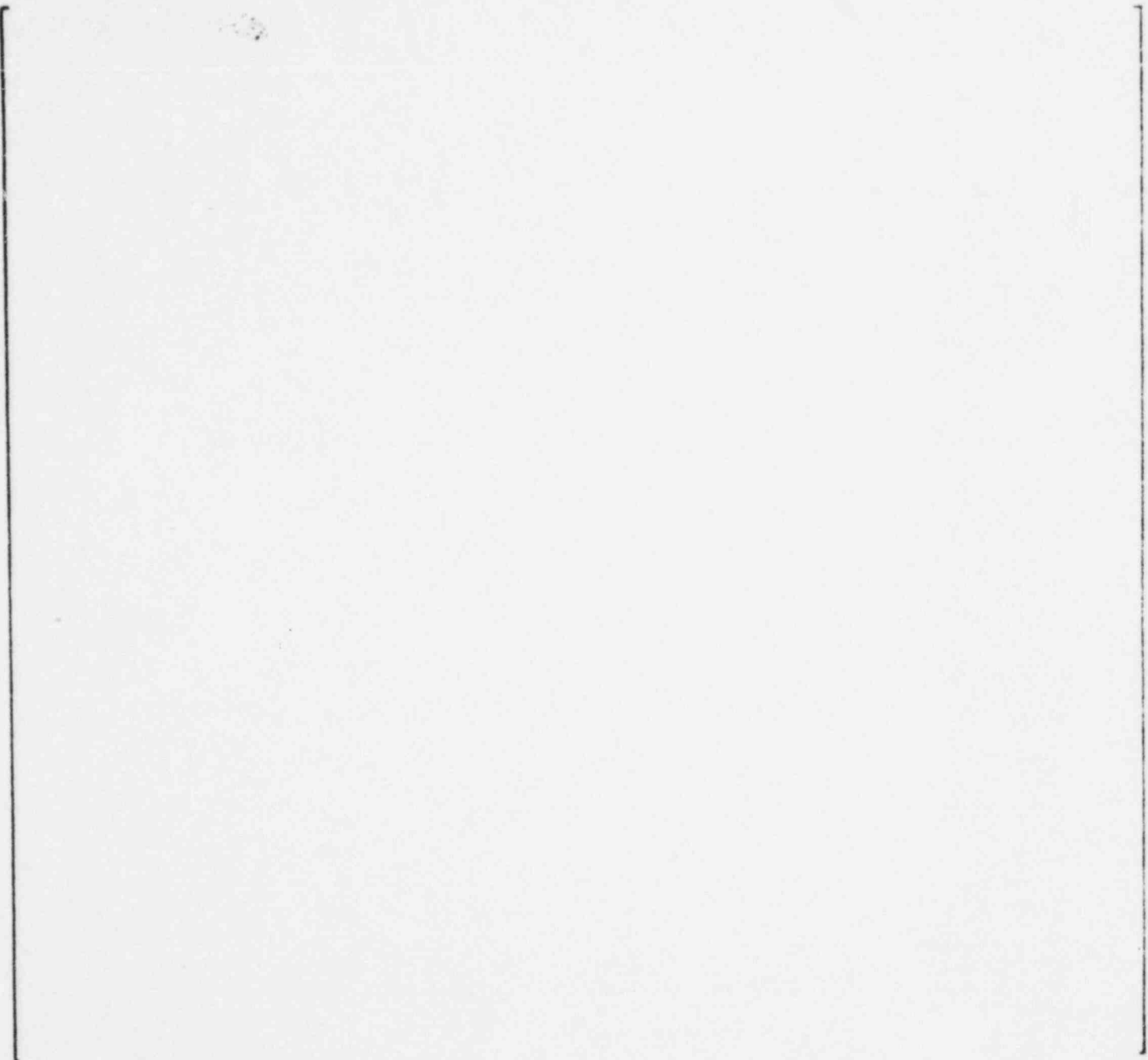


FIGURE 3-9  
EXIT PRESSURE DISTRIBUTIONS USED IN SENSITIVITY STUDY

Operating Conditions	Units	Range
Axial Shape Index	*	$-0.55 \leq \text{A.S.I.} \leq 0.55$
Inlet Temperature	°F	$465 \leq T_{in} \leq 580$
System Pressure	psia	$1750 \leq P_{sys} \leq 2400$
System Flow	% design <sup>†</sup>	$77 \leq w \leq 120$

Notes

\*See note (1) on Table 3-3 for definition of axial shape index

†Thermal Margin design flow = 370,000 gpm

TABLE 3-1: RANGES OF OPERATING CONDITIONS FOR WHICH RESPONSE SURFACE IS VALID

Stage 1 Channel Number	Inlet Flow Fraction*	
	Nominal	Perturbed

$$*Inlet\ Flow\ Fraction = \frac{Assembly\ Inlet\ Mass\ Velocity}{Core\ Average\ Mass\ Velocity}$$

TABLE 3-2: NOMINAL AND PERTURBED FLOW FOR ESTABLISHING SENSITIVITY OF FLOW DISTRIBUTION EFFECTS ON MDNBR TO OPERATING CONDITIONS

State Parameters				MDNBR			
Axial Shape Index	Pressure	Inlet Temperature	System Flow	Nominal Flow	Perturbed Flow*	$\Delta$	% Change
(1)	psia	°F	% design	-	-	(2)	(3)
-0.07	2200	550	100				
-0.02	2200	550	100				
0.00	2200	550	100				
0.317	2200	550	100				
0.337	2200	550	100				
0.444	2200	550	100				
0.527	2200	550	100				
-0.070	2400	580	120				
-0.070	1750	580	120				
-0.070	2400	465	120				
-0.070	1750	465	120				
-0.070	2400	580	77				
-0.070	1750	580	77				
-0.070	2400	465	77				
-0.070	1750	465	77				
0.337	1750	580	77				
0.337	1750	465	77				
0.337	1750	580	120				

$$(1) \text{ Axial Shape Index} = \frac{\int_{-L/2}^0 F_z dz - \int_0^{L/2} F_z dz}{\int_{-L/2}^{L/2} F_z dz}$$

core average  
 $F_z$  = axial peaking factor  
 $o$  = core midplane  
 $L$  = active core length

(2)  $\Delta$ MDNBR = "Nominal" MDNBR - "Perturbed" MDNBR

(3) % Change in MDNBR = ( $\Delta$ MDNBR / Nominal MDNBR) x 100

\*see Table 3-2

TABLE 3-3: FLOW PERTURBATION EFFECTS AT VARIOUS OPERATING CONDITIONS

M D N B R				
AXIAL SHAPE INDEX	NOMINAL	ENTHALPY RISE FACTOR APPLIED	$\Delta$	% CHANGE
(1)	-	-	(2)	(3)
-0.527				
-0.359				
-0.070				
-0.020				
0.00(C)*				
0.00(S)*				
0.337				
0.444				
0.527				
-0.317				
-0.162				
0.317				

\*Both a cosine (denoted by "C") and saddle (denoted by "S") Axial Shape were used for 0.00 A.S.I.

OPERATING CONDITIONS:

Inlet Pressure = 2200 psia  
 Inlet Temperature = 550°F  
 System Flow = 100% design

(1) }  
 (2) } See Notes on Table 3-3  
 (3) }

TABLE 3-4: SENSITIVITY OF ENTHALPY RISE FACTOR EFFECTS TO AXIAL SHAPE INDEX (ISOLATED HOT ASSEMBLY MODEL)



STATE PARAMETERS				M D N B R			
Axial Shape Index	Pressure	Inlet Temperature	System Flow	Nominal	Enthalpy Rise Factor Applied	$\Delta$	% Change
(1)	psia	$^{\circ}$ F	% design	-	-	(2)	(3)

(1) }  
 (2) } See Notes on Table 3-3  
 (3) }

TABLE 3-5: SENSITIVITY OF ENTHALPY RISE FACTOR EFFECTS TO OPERATING CONDITIONS (Isolated Hot Assembly Model)

M D N B R				
Axial Shape Index	Nominal	Enthalpy Rise Factor Applied	$\Delta$	% Change
(1)	-	-	(2)	(3)

OPERATING CONDITIONS

Pressure = 2200 psia  
 Inlet Temperature = 550°F  
 System Flow = 100% design

(1) }  
 (2) } See Notes on Table 3-3  
 (3) }

TABLE 3-6: SENSITIVITY OF ENTHALPY RISE FACTOR EFFECTS TO AXIAL SHAPE INDEX (Core Wide Analysis)

STATE PARAMETERS				MDNBR			
Axial Shape Index	Pressure	Inlet Temperature	System Flow	Nominal	Reduced Pitch	$\Delta$	% Change
(1)	psia	$^{\circ}\text{F}$	% design	-	-	(2)	(3)

(1) }  
 (2) } See Notes on Table 3-3  
 (3) }

TABLE 3-7: SENSITIVITY OF SYSTEMATIC PITCH REDUCTION EFFECTS TO OPERATING CONDITIONS

STATE PARAMETERS				
System Parameter	Axial Shape Index	Pressure	Inlet Temperature	System Flow
	(1)	psia	°F	% Design
Inlet Flow Distribution	[			]
Enthalpy Rise Factor				
Systematic Pitch Reduction				

(1) See note on Table 3-3

TABLE 3-8: STATE PARAMETERS WHICH MAXIMIZE MDNBR SENSITIVITY TO SYSTEM PARAMETERS

Axial Shape Index	Flow Split Reduction*	MDNBR	Change in MDNBR
[			]

[ ]

TABLE 3-9: MDNBR SENSITIVITY TO INLET FLOW DISTRIBUTION

Axial Shape Index	Exit Pressure Distribution	MDNBR	Change In MDNBR
0.444	nominal	[	]
0.444	extreme		
-0.359	nominal		
-0.359	extreme		

TABLE 3-10: SENSITIVITY OF MDNBR TO EXIT PRESSURE DISTRIBUTION

CYCLE	1	2	3	4	5
BATCH	A,B,C	D	E	F	G
OMAHA					
MILLSTONE					
CC #2					
CC #1					
ST. LUCIE 1					
MAINE YANKEE					

- Mean
- Standard Deviation
- Standard Deviation of the Mean

Note: Nominal Clad O.D. = 0.44 inches

TABLE 3-11 AS BUILT CLAD O.D. (inches) DATA FOR 14 X 14 FUEL

Span Number	Fort Calhoun	Millstone	Calvert Cliffs I	Maine Yankee	Calvert Cliffs II			
					C-010	C-012	C-013	C-105
8								
7								
6								
5								
4								
3								
2								
1								

Mean → xxxx(xxx) ← number of measurements  
 xxxx ← standard deviation of mean

TABLE 3-12: AS-BUILT GAP WIDTH DATA (INCHES)



#### 4.0 MDNBR Response Surface

A response surface is a functional relationship which involves several independent variables and one dependent variable. The surface is created by fitting the constants of an assumed functional relationship to data obtained from experiments.

The response surface provides a convenient means by which accurate estimates of a complex or unknown function response may be obtained. Since the response surface is a relatively simple expression, it may be applied in analytic techniques where more complex functions would make an analytic solution intractable.

In the present application, a single detailed TORC analysis is treated as an "experiment". A carefully selected set of detailed TORC "experiments" is conducted, and a functional relationship is fitted to the MDNBR results. This response surface is then used in conjunction with Monte Carlo techniques to combine probability distribution functions (p.d.f.'s) for each of the independent variables into a resultant MDNBR p.d.f..

#### 4.1 TORC Model Used

The inlet flow distribution (shown in Fig. 3-8) is compared with radial power distributions for the Calvert Cliffs Unit 1 and Unit 2 reactors to determine the limiting location for DNB analysis. For the purpose of generating the response surface, the limiting location is defined as the assembly in which the impact of system parameter uncertainties on MDNBR is the greatest. The core wide and limiting assembly radial power distributions used to generate the response surface are shown in Fig. 4-1 and 4-2, respectively.

The first stage TORC model used in this analysis is shown in Fig. 3-5. The limiting assembly occurs in channel  $f_1$  of this model. Second and third stage models used in this analysis are shown in Fig. 4-3 and 4-4 respectively.

#### 4.2 Variables Used

A careful examination of the sources of uncertainty discussed in Section 3 shows that several of these sources of uncertainty can be omitted from the response surface.

The state variables mentioned in section 3.1 are treated in part 1 of this report (4-1).

As explained in Section 3.2, inherent conservatism in the calculation of radial peaking factors makes the need to account for uncertainty in the radial power distribution used in DNB analyses unnecessary. Hence, the radial power distribution was omitted from the response surface.

The sensitivity study discussed in Section 3.4 indicates that large perturbations in the exit pressure distribution have negligible effect on the predicted MDNBR. Thus, the exit pressure distribution is not included in the response surface.

The heat flux factor ( $F_{q''}$ ) is applied to the MDNBR calculated by TORC in the following manner:

$$\text{MDNBR} = \frac{\text{MDNBR}_{\text{TORC}}}{F_{q''}} \quad (4.1)$$

Since the functional relationship between MDNBR and  $F_{q''}$  is known, the heat flux factor is not used in generating the response surface. Instead, this factor is combined with the resultant surface, as explained in section 4.5.

A method has already been developed (4-2) to account for rod bow uncertainty. No rod bow effects are included in the response surface. Instead, the rod bow penalty found with existing methods (4-2) is applied to the design limit MDNBR found in the present analysis.

The calculational uncertainty associated with MDNBR predictions found with the TORC/CE-1 package is implicitly included in the CHF distribution uncertainty, as explained in Sections 3.10 and 3.11. Hence no explicit allowance for code uncertainty is included in the response surface.

The system parameters included as variables in the response surface are listed in Table 4-1.

#### 4.3 Experiment Design

An orthogonal central composite experimental design (4-3) is used to generate the response surface applied in this study. The total number of experiments needed to generate a response surface using this experiment design is

$$2^k + 2k + 1$$

where  $k$  is the number of variables to be considered. The desired response surface consists of seven variables, hence 143 "experiments" or detailed TORC analyses were needed for a full orthogonal central composite design. The results of these experiments may then be manipulated by means of the least squares estimator

$$\underline{b} = \{n' \ n\}^{-1} \{n'\} \underline{z} \quad (4.2)$$

where  $z$  is the vector of experimental results,  
to yield the coefficients which define the response surface

$$z = \text{MDNBR}_{RS} = b_0 + \sum_{i=1}^7 b_i n_i + \sum_{i=1}^7 b_{ii} (n_i^2 - c) + \sum_{i=1}^7 \sum_{\substack{j=1 \\ i < j}}^7 b_{ij} n_i n_j \quad (4.3)$$

In the above equations, the  $n_i$  are coded values of the system parameters ( $x_i$ ) to be treated in the response surface, as indicated in Table 4-1. The  $b_i$  represent the constants found from the TORC results by means of Eq. 4.2, and  $c$  is a constant determined by the number of experiments conducted.

The number of TORC analyses needed to generate the response surface could be reduced significantly if some of the interaction effects (i.e.  $b_{ij} n_i n_j$ ) were neglected.

#### 4.4 Design Matrix

The set of experiments used to generate the response surface is referred to as the design matrix. This matrix, in coded form, comprises the second through eighth columns of the  $n$  matrix cited in Eq. (4.2). Both coded and uncoded versions of the design matrix used in this study are presented in Appendix A along with resultant MDNBR values. The design matrix was constructed such that each independent variable included in the response surface extends just beyond the  $2\sigma$  range of its associated p.d.f.

#### 4.5 Response Surface

Equation (4.2) was solved numerically using the data in Appendix A.

Constants for the response surface as given by Eq.(4.3) are presented in Table 4-2. Comparisons made between TORC predicted MDNBR and response surface predictions show excellent agreement. The 95% confidence estimate of the response surface standard deviation is 0.00377.

The heat flux factor is included analytically in the response surface by combining Eq. (4.0) with Eq. 4.3). The final relationship is given by

$$\text{MDNBR} = \frac{1}{F_q''} \left\{ b_0 + \sum_{i=1}^7 b_i n_i + \sum_{i=1}^7 b_{ii} (n_i^2 - c) + \sum_{i=1}^7 \sum_{\substack{j=1 \\ i < j}}^7 b_{ij} n_i n_j \right\} \quad (4-4)$$

The coefficient of determination,  $r$ , provides an indication of how well the response surface explains the total variation in the response variable (4-4). When  $r=1$ , a true model has been found. The  $r$  value associated with the response surface generated in this work is 0.9995, which indicates that this response surface is a good model.

Another indication of model performance is provided by the standard error of estimate (4-5). The standard error for the response surface is 0.003396. The relative error is 0.29%, indicating that this model performs well.



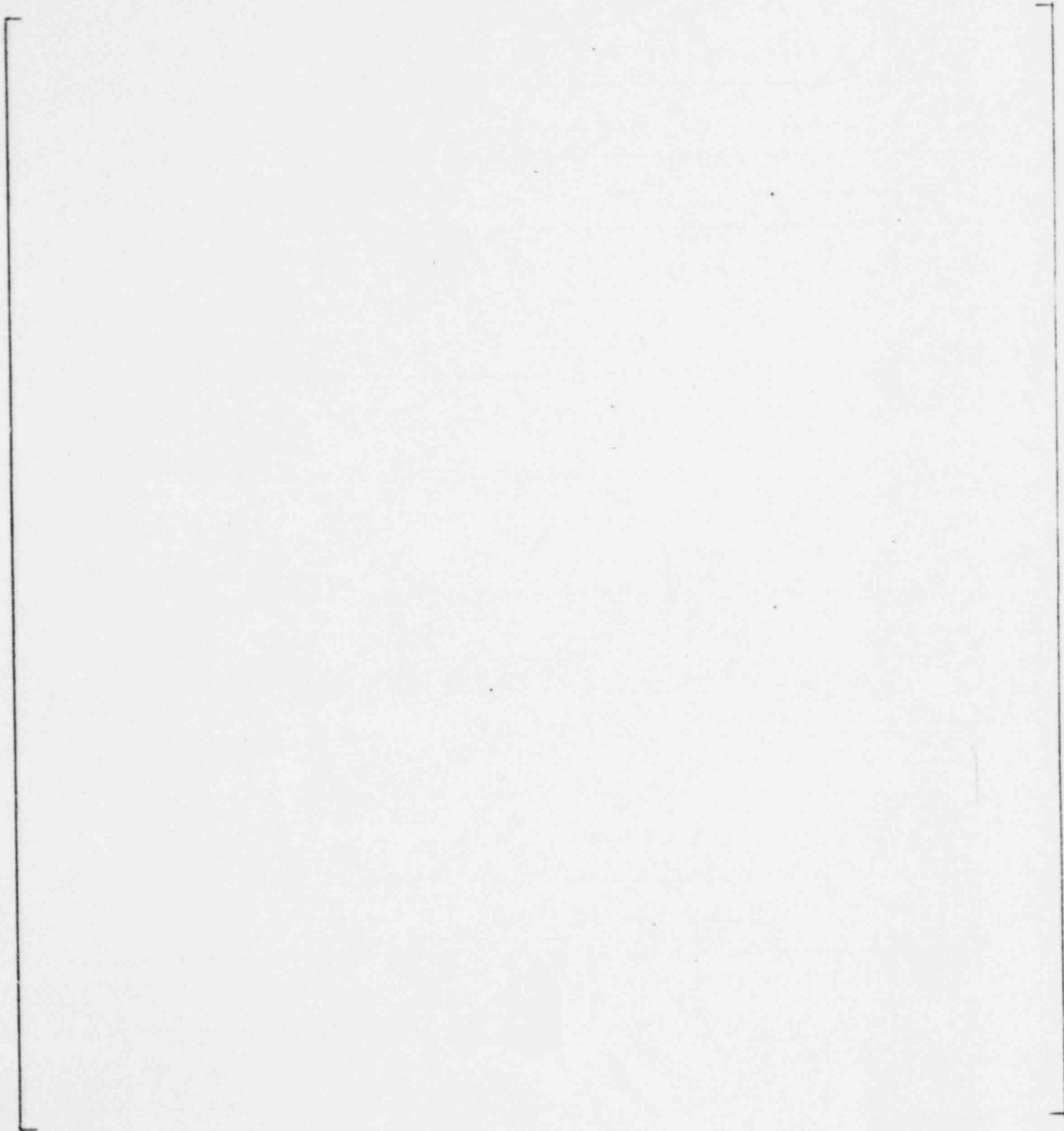


Figure 4-2  
HOT ASSEMBLY RADIAL POWER DISTRIBUTION USED TO  
GENERATE RESPONSE SURFACE

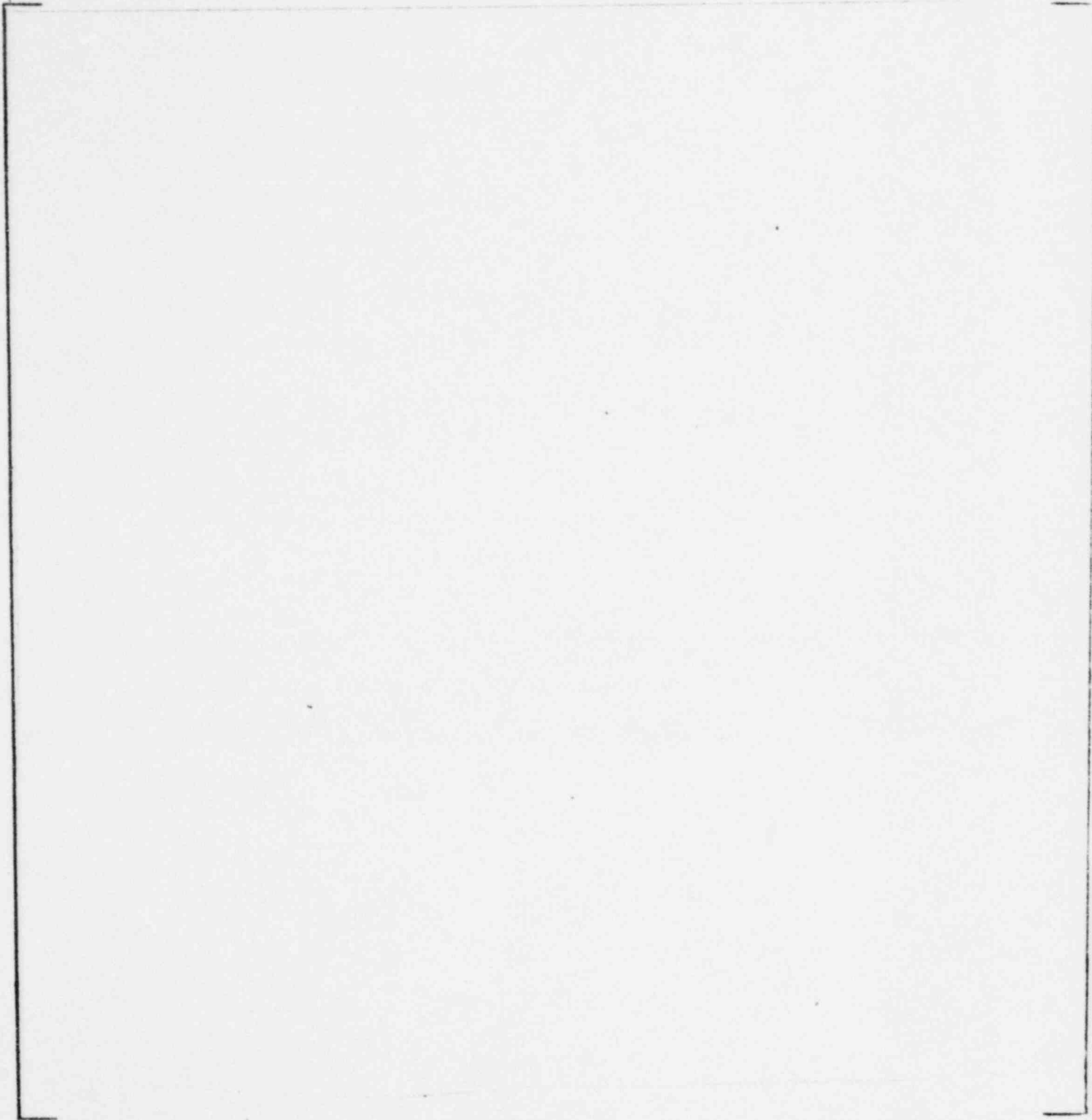


Figure 4-3

INTERMEDIATE (2ND STAGE) TORC MODEL USED IN GENERATING  
RESPONSE SURFACE

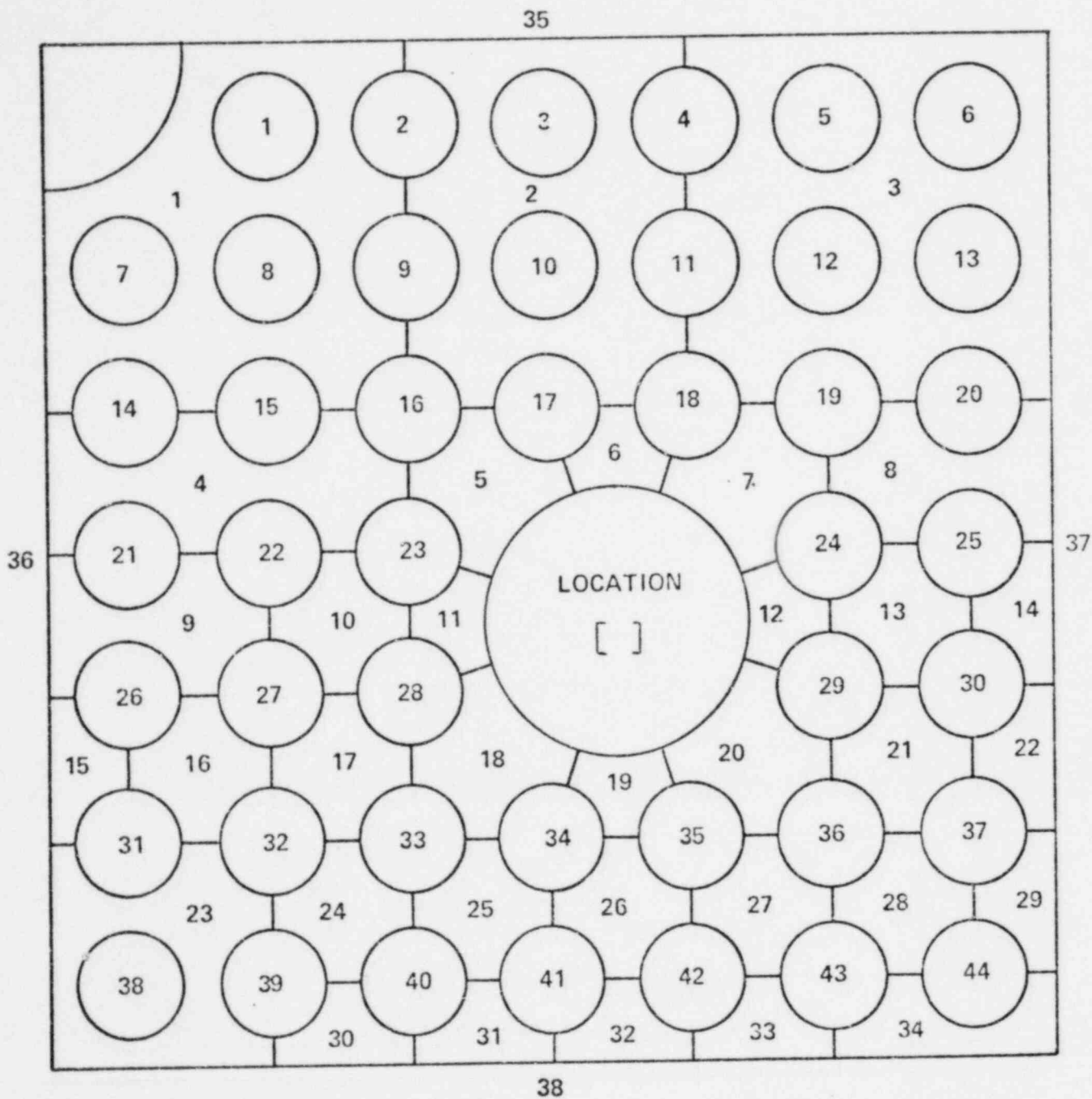


Figure 4-4  
 SUBCHANNEL (3RD STAGE) TORC MODEL USED IN GENERATING  
 RESPONSE SURFACE



System Parameter	Variable	Index(i)	Coded Variable**	
			$\alpha$	$\beta$
hot assembly inlet flow factor (channel[4*])	x <sub>1</sub>	1	[	]
channel[3*]inlet flow factor	x <sub>2</sub>	2		
channel[5*]inlet flow factor	x <sub>3</sub>	3		
channel[10*]inlet flow factor	x <sub>4</sub>	4		
enthalpy rise factor	x <sub>5</sub>	5	1.0001	0.0119
systematic pitch	x <sub>6</sub>	6	[	]
systematic clad O.D.	x <sub>7</sub>	7		

\*channel numbers refer to Figure 3-5

\*\*variables coded according to relation  $\eta_i = \frac{x_i - \alpha_i}{\beta_i}$  where the  $\alpha_i$  are chosen such that  $\eta_i = 0$  at nominal conditions, and the  $\beta_i$  are chosen such that the range of the response surface will include  $\sim 2\sigma$  ranges of each of the system parameters

TABLE 4-1: STATE PARAMETERS INCLUDED AS VARIABLES IN THE RESPONSE SURFACE

$$\text{MDNBR}_{\text{RS}} = b_0 + \sum_{i=1}^7 b_i \eta_i + \sum_{i=1}^7 b_{ii} (\eta_i^2 - c) + \sum_{\substack{i=1 \\ i < j}}^7 \sum_{j=1}^7 b_{ij} \eta_i \eta_j$$

TABLE 4-2: COEFFICIENTS FOR MDNBR RESPONSE SURFACE

## 5.0 Combination of Probability Distribution Functions

The MDNBR response surface discussed in Section 5 is applied in Monte Carlo methods to combine numerically the system parameter probability distribution functions (p.d.f.'s) discussed in Section 3 with the CHF correlation uncertainty. A new 95/95 MDNBR limit is then selected from the resultant p.d.f. This new limit includes the effect of system parameter uncertainties and thus may be used in conjunction with a best estimate design TORC model.

### 5.1 Method

The SIGMA code applies Monte Carlo and stratified sampling techniques to combine arbitrary p.d.f.'s numerically (5-1). This code is used with the response surface to combine system parameter p.d.f.'s with the CE-1 CHF correlation p.d.f. into a resultant MDNBR p.d.f. The methods used to achieve this combination are discussed below.

The effect of system parameter uncertainties on MDNBR is combined with the effect of uncertainty in the CHF correlation by computing a  $\Delta$ MDNBR caused by deviation of the system parameters from nominal:

$$\Delta \text{MDNBR} = \text{MDNBR}_{RS} - \text{MDNBR}_{NOM} \quad (5.1)$$

where  $\text{MDNBR}_{RS}$  is the MDNBR found by substituting the set of system parameters into the response surface and  $\text{MDNBR}_{NOM}$  is the MDNBR value predicted by the response surface with nominal system parameters. A point is then randomly chosen from the CHF correlation p.d.f. and combined with the  $\Delta$ MDNBR from Eq. (5.1) to yield a MDNBR value:

$$\text{MDNBR} = \text{MDNBR}_{CHF} + \Delta \text{MDNBR} \quad (5.2)$$

This process is repeated by the SIGMA code for 2000 randomly selected sets of system parameters and randomly selected points from the CHF correlation p.d.f., and a resultant MDNBR p.d.f. is generated.

The system parameter p.d.f.'s input to SIGMA are listed in Table 5-1. Both "best estimate" and 95% confidence estimates of the standard deviation are included. Standard deviations at the 95% confidence level are input to SIGMA to ensure that the standard deviation of the resultant MDNBR p.d.f. is at least at the 95% confidence limit.

## 5.2 Results

The resultant MDNBR p.d.f. is shown in Fig. 5-1. The mean and standard deviation of this p.d.f. are 0.988 and 0.099451, respectively. As Fig. 5-1 indicates, the resultant MDNBR p.d.f. approximates a normal distribution.

## 5.3 Analytic Comparison

An approximate value of the standard deviation of the resultant MDNBR p.d.f. may be found by analytic methods. These methods are based upon the assumption that the uncertainties are small deviations from the mean (5-2). Given a functional relationship

$$y = f(x_1, x_2, \dots, x_n) \quad (5.3)$$

the effects of small perturbations in  $x$  on  $y$  may be found from

$$\Delta y = dy = \frac{\partial f}{\partial x_1} \Delta x_1 + \frac{\partial f}{\partial x_2} \Delta x_2 + \dots + \frac{\partial f}{\partial x_n} \Delta x_n \quad (5.4)$$

Hence, if several normal distributions are combined by the relationship expressed in Eq.(5.3), the variance of the resultant p.d.f. is

$$\sigma_y^2 = \left(\frac{\partial f}{\partial x_1}\right)^2 \sigma_{x_1}^2 + \left(\frac{\partial f}{\partial x_2}\right)^2 \sigma_{x_2}^2 + \dots + \left(\frac{\partial f}{\partial x_n}\right)^2 \sigma_{x_n}^2 \quad (5.5)$$

where the partial derivatives are evaluated at the mean values of the  $x_i$ 's.

The response surface relates MDNBR to system parameters by the relationship found on Table 4-2:

$$\text{MDNBR}_{RS} = b_0 + \sum_{i=1}^7 b_i n_i + \sum_{i=1}^7 b_{ii} (n_i^2 - c) + \sum_{i=1}^7 \sum_{\substack{j=1 \\ i < j}}^7 b_{ij} n_i n_j \quad (5.6)$$

where

$$n_i = \frac{x_i - \alpha_i}{\beta_i} \quad (5.7)$$

Applying Eq. 5.5 to the response surface yields the following expression for the variance:

$$\sigma_{RS}^2 = \sum_{i=1}^7 \left( \frac{\partial(\text{MDNBR})}{\partial n_i} \frac{\partial n_i}{\partial x_i} \right)^2 \sigma_{x_i}^2 \quad (5.8)$$

Differentiating Eq. (5.6) and (5.7) with respect to  $n_i$  and  $x_i$ :

$$\frac{\partial \text{MDNBR}}{\partial n_i} = b_i + 2b_{ii} n_i + \sum_{j=i+1}^7 b_{ij} n_j \quad (5.9)$$

$$\frac{\partial n_i}{\partial x_i} = \frac{1}{\beta_i} \quad (5.10)$$

Substituting Eq.(5.9) and (5.10) into Eq.(5.8) results in a relation between the resultant MDNBR variance and the system parameter variances:

$$\sigma_{RS}^2 = \sum_{i=1}^7 (b_i + 2b_{ii} n_i + \sum_{j=i+1}^7 b_{ij} n_j)^2 \left( \frac{\sigma_{x_i}}{\beta_i} \right)^2 \quad (5.11)$$

This equation is simplified when evaluated at the mean values of the  $n_i$ : (i.e.  $n_i=0$ )

$$\sigma_{RS}^2 = \sum_{i=1}^7 b_i^2 \frac{\sigma_{x_i}^2}{\beta_i^2} \quad (5.12)$$

The CHF correlation p.d.f. and system parameter p.d.f.'s are related to the resultant MDNBR in Eq.(5.1) and Eq.(5.2), the heat flux factor is related by Eq.(4.1). The resultant MDNBR variance is given by

$$\frac{\sigma_{\text{MDNBR}}^2}{\mu_{\text{MDNBR}}^2} = \frac{\sigma_{RS}^2 + \sigma_{\text{CHF}}^2}{\mu_{\text{CHF}}^2} + \frac{\sigma_{\text{Fq}}^2}{\mu_{\text{Fq}}^2} \quad (5.13)$$

Substituting values from Tables 4-1, 4-2, 5-1, and Section 4.5 into Eq. (5.11) and Eq (5.13) yields

$$\sigma_{\text{MDNBR}} = 0.09923$$

which is in excellent agreement with the value predicted by the SIGMA code simulation using the response surface.

DISTRIBUTION	MEAN	STANDARD DEVIATION	
		BEST ESTIMATE	95% CONFIDENCE
hot assembly inlet flow factor (channel[ ])	[		]
channel[ ] inlet flow factor			
channel[ ] inlet flow factor			
channel[ ] inlet flow factor			
enthalpy rise factor	1.0	-	.0100 <sup>†</sup>
systematic pitch (inches)	[		]
systematic clad O.D. (inches)			
heat flux factor	1.0	-	.0150 <sup>**</sup>
CE-1 CHF Correlation	.998	.0676	.07384

\*channel numbers refer to Figure 3-5

<sup>†</sup>entire fuel pin population was sampled, hence >95% confidence

<sup>\*\*</sup>standard deviation based upon tolerance limits, hence >95% confidence

TABLE 5-1: PROBABILITY DISTRIBUTION FUNCTIONS COMBINED BY SIGMA

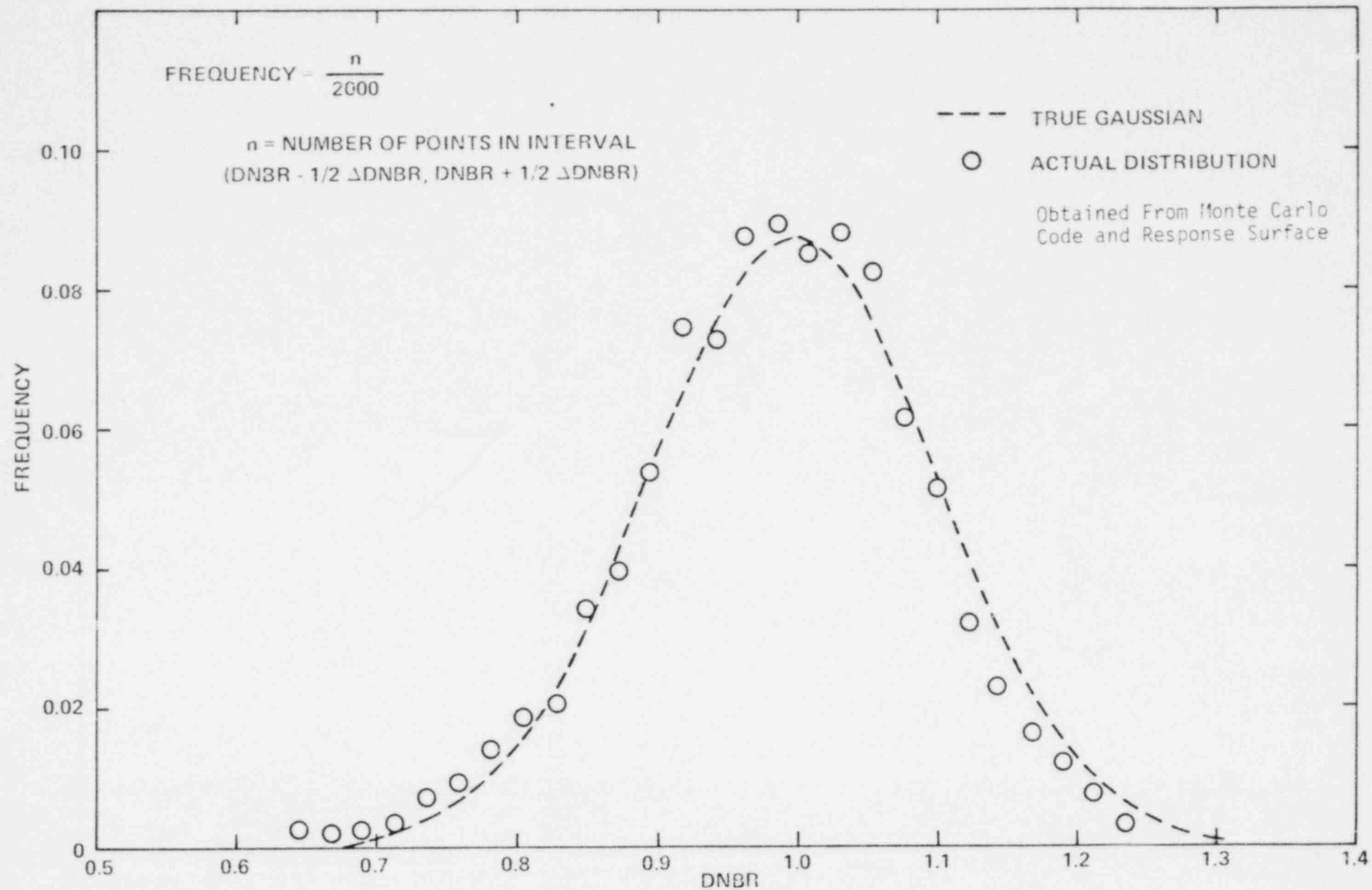


Figure 5-1  
RESULTANT MDNBR PROBABILITY DISTRIBUTION FUNCTION

## 6.0 Application to Design Analyses

This section discusses the application of the statistically derived MDNBR p.d.f. to design analyses. Deterministic methodology (6-1) involves use of a design model for TORC analysis which includes deterministic allowances for system parameter uncertainties. These deterministic penalties are replaced with a higher MDNBR limit in the statistical methodology. This higher MDNBR limit is used with a "best estimate" design model in thermal margin analyses.

### 6.1 Statistically Derived MDNBR Limit

The MDNBR p.d.f. described in Section 5.0 is a normal distribution having a mean of .9875 and a standard deviation of 0.099451. This standard deviation is at least at the 95% confidence level. A comparison of TORC results and response surface predictions indicates that the  $1\sigma$  error associated with the response surface is  $\sigma_s = 0.003396$ ; at the 95% confidence level, this value is  $\sigma_{s95} = (.003396 \times \sqrt{142/115.461}) = .00377$ . (See Eqn. 2-3 of Ref. 6 5)

The MDNBR standard deviation was found to be 0.099451 by means of Monte Carlo methods. Since a finite number of points (2000) were used in these methods, a correction must be applied to the calculated value. The resultant MDNBR standard deviation, adjusted for the finite sample size used is  $(0.099451 \times \sqrt{1999/1896.131}) = 0.10211$ . The root sum square of this adjusted MDNBR standard deviation and the response surface standard deviation at the 95% confidence level is

$\sigma_{tot} = \sqrt{(0.10211)^2 + (0.00377)^2} = 0.10218$ . The corresponding 95% confidence estimate of the mean is

$$(.9875 + (1.645 \times 0.10211) / \sqrt{1999}) = 0.991. \text{ (See Eqn. 2-2 of Ref. 6 5)}$$

Since the resultant MDNBR p.d.f. is a normal distribution, as shown in Figure 5-1, the one-sided 95% probability limit is  $1.645\sigma$ . Hence there is a 95% probability with at least 95% confidence that the limiting fuel pin will not experience DNB if the best estimate design model TORC calculation yields a MDNBR value greater than or equal to  $(0.991 + 1.645 \times 0.10218) = 1.16$ .

### 6.2 Adjustments to Statistically Derived MDNBR Limit

The statistical MDNBR limit derived in Section 6.1 contains no allowance for the adverse impact on DNBR of fuel rod bowing. CE has applied an NRC method for taking rod bow into account in DNBR calculations (6-2). This application shows that the maximum penalty occurs at fuel end-of-life. For 14x14 fuel, this penalty is 0.6% in MDNBR. Thus, the new limit, including an allowance for rod bow is  $(1.006 \times 1.160)$  or 1.167.

The NRC has not yet completed review of the application of the CE-1 CHF correlation (6-3) to non-uniform axial heat flux shape data (6-4). Consequently, a 5% penalty was applied to the 1.13 MDNBR limit by the NRC. The interim MDNBR limit for use with the CE-1 CHF correlation, pending NRC approval of CE's non-uniform axial heat flux shape data, is 1.19. For the purposes of this study, a conservative application of this penalty is to shift the mean of the MDNBR p.d.f. by 0.06. This shift results in a MDNBR limit of 1.227.

Thus the new MDNBR limit which contains allowance for uncertainty in the CHF correlation and system parameters as well as a rod bow penalty and the interim 5% penalty on the CE-1 correlation imposed by the NRC is 1.23.



### 6.3 Application to TORC Design Model

Statistical combination of system parameter uncertainties into the MDNBR limit precludes the need for deterministic application of penalty factors to the design TORC model. The design TORC model used with the new MDNBR limit of 1.23 consists of best estimate system parameters with no engineering factors or other adjustments to accommodate system parameter uncertainties. The inlet flow split will, however, continue to be chosen such that the best estimate design TORC model will yield accurate or conservative MDNBR predictions when compared with MDNBR values from detailed TORC analyses(6-1).

## 7.0 Conclusions

Use of a 1.23 MDNBR limit with a best estimate design TORC model for the Calvert Cliffs Unit 1 and Unit 2 cores will ensure with at least 95% probability and 95% confidence, that the hot pin will not experience a departure from nucleate boiling. The 1.23 MDNBR limit includes explicit allowances for system parameter uncertainties, CHF correlation uncertainty, rod bow, and the 5% interim penalty imposed by the NRC on the CE-1 CHF correlation.

### 7.1 Conservatisms in the Methodology

Several conservatisms are included in the present application. The significant conservatisms include:

- i) combination of system parameter p.d.f.'s at the 95% confidence level to yield a resultant MDNBR at a 95% + confidence level
- ii) use of pessimistic (generic) system parameter p.d.f.'s
- iii) derivation of the new MDNBR limit such that it applies to both 4-pump operation and seized rotor analyses
- iv) use of the single most adverse set of state parameters to generate the response surface
- v) application of the 5% interim penalty imposed by the NRC on the CE-1 CHF correlation

8.0 References

8.1 Section 1.0 References

(1-1) "Report on Statistical Combination of Uncertainties Methodology, Part 1, C-E Calculated Local Power Density and Thermal Margin/Low Pressure LSS for Calvert Cliffs Units I and II", CEN-124(B)-P, December 13, 1979

8.2 Section 2.0 References

(2-1) "TORC Code: Verification and Simplified Modeling Models", CENPD-206-P, January 1977.

(2-2) "TORC Code: A Computer Code for Determining the Thermal Margin of a Reactor Core", CENPD-161-P, July 1975.

(2-3) "C-E Critical Heat Flux: Critical Heat Flux Correlation for C-E Fuel Assemblies with Standard Grids, Part 1: Uniform Axial Power Distribution", CENPD-162-P, September 1976.

8.3 Section 3.0 References

(3-1) "TORC Code: A Computer Code for Determining the Thermal Margin of a Reactor Core, CENPD-161-P, July 1975, pp. 5-1 to 5-8.

(3-2) "Report on Statistical Combination of Uncertainties Methodology, Part 1, C-E Calculated Local Power Density and Thermal Margin/Low Pressure LSS for Calvert Cliffs Units I and II", CEN-124(B)-P, December 13, 1979.

(3-3) Combustion Engineering Standard Safety Analysis Report, (System 80), Docket #STN-50-470F, October 26, 1979, Fig. 4.4-7.

(3-4) *ibid*, Subsection 4.4.2.2.2.2.C.

(3-5) W. R. Cadwell, "PDQ-7 Reference Manual", WAPD-TM-678, January, 1968, Westinghouse Electric Corporation.

(3-6) A. Jonsson, et al., "Core Physics Validation for the Combustion Engineering PWR", Combustion Engineering Technical Paper TIS 6368 Presented at the American Nuclear Society Winter Meeting, November 12-16, 1979, San Francisco.

(3-7) Green & Bourne, "Reliability Technology", Wiley-Interscience, a division of John Wiley & Sons Ltd., p. 326.

(3-8) "Fuel and Poison Rod Bowing", CENPD-225-P, October 1976.

(3-9) "Fuel and Poison Rod Bowing-Supplement 3", CENPD-225-P, Supplement 3, June 1979.

(3-10) Letter from D. B. Vassallo (NRC) to A. E. Scherer (C-E), June 12, 1978.

(3-11) "C-E Critical Heat Flux: Critical Heat Flux Correlation for C-E Fuel Assemblies with Standard Spacer Grids, Part 1: Uniform Axial Power Distribution", CENPD-162-P, September 1976.

(3-12) "C-E Critical Heat Flux: Critical Heat Flux Correlation for C-E Fuel Assemblies with Standard Spacer Grids, Part 2: Nonuniform Axial Power Distribution", CENPD-207-P, June 1976

(3-13) "TORC Code: Verification and Simplified Modeling Methods", CENPD-206-P, January 1977.

#### 8.4 References for Section 4

(4-1) "Report on Statistical Combination of Uncertainties Methodology Part 1, C-E Calculated Local Power Density and Thermal Margin/Low Pressure LSSS for Calvert Cliffs Units I and II", CEN-124(B)-P, December 13, 1979.

(4-2) "Fuel and Poison Rod Bowing, Supplement 3", CENPD-225-P, Supplement 3-P, June, 1979.

(4-3) R. H. Myers, Response Surface Methodology, Allyn and Bacon, Inc., Boston, 1971.

(4-4) N. R. Draper, H. Smith, Applied Regression Analysis, John Wiley & Sons, New York, 1966, p. 62.

(4-5) *ibid.*, p. 118.

#### 8.5 References for Section 5

(5-1) F. J. Berte, "The Application of Monte Carlo and Bayesian Probability Techniques to Flow Prediction and Determination", Combustion Engineering Technical Paper TIS-5122, presented at the Flow Measurement Symposium, sponsored by the National Bureau of Standards, Gaithersburg, Maryland, February 23-25, 1977.

(5-2) E. L. Crow, F. A. Davis, M. W. Maxfield, Statistics Manual, Dover Publications, Inc., New York, 1960.

#### 8.6 References for Section 6

(6-1) "TORC Code: Verification and Simplified Modeling Methods", CENPD-206-P, January 1977.

(6-2) "Fuel and Poison Rod Bowing, Supplement 3", CENPD-225-P, Supplement 3-P, June 1979.

(6-3) "C-E Critical Heat Flux: Critical Heat Flux Correlation for C-E Fuel Assemblies with Standard Spacer Grids, Part 1: Uniform Axial Power Distribution", CENPD-162-P, September, 1976.

(6-4) "C-E Critical Heat Flux: Critical Heat Flux Correlation for C-E Fuel Assemblies with Standard Spacer Grids, Part 2: Nonuniform Axial Power Distribution", CENPD-207-P, June, 1976.

- (6-5) "Statistical Combination of Uncertainties Methodology Part 1:  
C-E Calculated Local Power Density and Thermal Margin/Low Pressure  
LSSS for Calvert Cliffs Units I and II," CEN-124(B)-P, December, 1979.

Appendix A: Detailed TORC Analyses Used  
To Generate Response Surface

An orthogonal central composite experiment design (A-1) was used to generate the response surface (R S) used in this study. All first order interaction effects (i.e.  $x_i x_j$  terms) were retained in the R S. The R S used in this study included seven variables. The coded set of detailed TORC analyses performed to generate the R S is presented in Table A-1; variables were coded as shown in Table 5-1. The actual values of the input parameters are presented in Table A-2 along with the resultant MDNBR values.

References

- (A-1) R. H. Myers, Response Surface Methodology, Allyn & Bacon, Inc., Boston, 1971, p. 133.

Case Number	Inlet Flow Factors				Enthalpy Rate Factor	Systematic Pitch	Systematic Clad G.P.
	Channel [ ]	Channel [ ]	Channel [ ]	Channel [ ]			
1	-1	-1	-1	-1	-1	-1	-1
2	-1	-1	-1	-1	-1	-1	1
3	-1	-1	-1	-1	-1	1	-1
4	-1	-1	-1	-1	-1	1	1
5	-1	-1	-1	-1	1	-1	-1
6	-1	-1	-1	-1	1	-1	1
7	-1	-1	-1	-1	1	1	-1
8	-1	-1	-1	-1	1	1	1
9	-1	-1	-1	1	-1	-1	-1
10	-1	-1	-1	1	-1	-1	1
11	-1	-1	-1	1	-1	1	-1
12	-1	-1	-1	1	-1	1	1
13	-1	-1	-1	1	1	-1	-1

\*channel numbers refer to Fig. 3-5

see Table 4-1 for coded relationships

Note: Coded values determined by methods described in Reference (A-1).

Table A-1: Coded Set of Detailed TORG Cases Used to Generate Response Surface

Case Number	Inlet Flow Factors				Enthalpy Rise Factor	Systematic Pitch	Systematic Clad O.D.
	Channel [ ]	Channel [ ]	Channel [ ]	Channel [ ]			
14	-1	-1	-1	1	1	-1	1
15	-1	-1	-1	1	1	1	-1
16	-1	-1	-1	1	1	1	1
17	-1	-1	1	-1	-1	-1	-1
18	-1	-1	1	-1	-1	-1	1
19	-1	-1	1	-1	-1	1	-1
20	-1	-1	1	-1	-1	1	1
21	-1	-1	1	-1	1	-1	-1
22	-1	-1	1	-1	1	-1	1
23	-1	-1	1	-1	1	1	-1
24	-1	-1	1	-1	1	1	1
25	-1	-1	1	1	-1	-1	-1
26	-1	-1	1	1	-1	-1	1

\*Channel numbers refer to Fig. 3-5

see Table 4-1 for coded relationships

Note: Code ' values determined by methods described in Reference (A-1).

Table A-1: Coded Set of Detailed TORC Cases Used to Generate Response Surface (con't.)



Case Number	Inlet Flow Factors				Enthalpy Rise Factor	Systematic Pitch	Systematic Clad O.F.
	Channel [ ]	Channel [ ]	Channel [ ]	Channel [ ]			
27	-1	-1	1	1	-1	1	-1
28	-1	-1	1	1	-1	1	1
29	-1	-1	1	1	1	-1	-1
30	-1	-1	1	1	1	-1	1
31	-1	-1	1	1	1	1	-1
32	-1	-1	1	1	1	1	1
33	-1	1	-1	-1	-1	-1	-1
34	-1	1	-1	-1	-1	-1	1
35	-1	1	-1	-1	-1	1	-1
36	-1	1	-1	-1	-1	1	1
37	-1	1	-1	-1	1	-1	-1
38	-1	1	-1	-1	1	-1	1
39	-1	1	-1	-1	1	1	-1

\*channel numbers refer to Fig. 3-5

see Table A-1 for coded relationships

Note: Coded values determined by methods described in Reference (A-1).

Table A-1: Coded Set of Detailed TORC Cases Used to Generate Response Surface (con't)

Case Number	Inlet Flow Factors				Enthalpy Rise Factor	Systematic Pitch	Systematic Crad O.D.
	Channel [ ]	Channel [ ]	Channel [ ]	Channel [ ]			
40	-1	1	-1	-1	1	1	1
41	-1	1	-1	1	-1	-1	-1
42	-1	1	-1	1	-1	-1	1
43	-1	1	-1	1	-1	1	-1
44	-1	1	-1	1	-1	1	1
45	-1	1	-1	1	1	-1	-1
46	-1	1	-1	1	1	-1	1
47	-1	1	-1	1	1	1	-1
48	-1	1	-1	1	1	1	1
49	-1	1	1	-1	-1	-1	-1
50	-1	1	1	-1	-1	-1	1
51	-1	1	1	-1	-1	1	-1
52	-1	1	1	-1	-1	1	1

\*channel numbers refer to Fig. 3-5

see Table 4-1 for coded relationships

Note: Coded values determined by methods described in Reference (A-1).

Table A-1: Coded Set of Detailed TORC Cases Used to Generate Response Surface (con't.)

Case Number	Inlet Flow Factors				Enthalpy Rise Factor	Systematic Pitch	Systematic Clad O.D.
	Channel [ ]	Channel [ ]	Channel [ ]	Channel [ ]			
53	-1	1	1	-1	1	-1	-1
54	-1	1	1	-1	1	-1	1
55	-1	1	1	-1	1	1	-1
56	-1	1	1	-1	1	1	1
57	-1	1	1	1	-1	-1	-1
58	-1	1	1	1	-1	-1	1
59	-1	1	1	1	-1	1	-1
60	-1	1	1	1	-1	1	1
61	-1	1	1	1	1	-1	-1
62	-1	1	1	1	1	-1	1
63	-1	1	1	1	1	1	-1
64	-1	1	1	1	1	1	1
65	1	-1	-1	-1	-1	-1	-1

\*channel numbers refer to fig. 3-5

see Table 4-1 for coded relationships

Note: Coded values determined by methods described in Reference (A-1).

Table A-1: Coded Set of Detailed TORG Cases Used to Generate Response Surface (con't.)

Case Number	Inlet Flow Factors				Enthalpy Rise Factor	Systematic Pitch	Systematic Clad O.D.
	Channel [ ]	Channel [ ]	Channel [ ]	Channel [ ]			
66	1	-1	-1	-1	-1	-1	1
67	1	-1	-1	-1	-1	1	-1
68	1	-1	-1	-1	-1	1	1
69	1	-1	-1	-1	1	-1	-1
70	1	-1	-1	-1	1	-1	1
71	1	-1	-1	-1	1	1	-1
72	1	-1	-1	-1	1	1	1
73	1	-1	-1	1	-1	-1	-1
74	1	-1	-1	1	-1	-1	1
75	1	-1	-1	1	-1	1	-1
76	1	-1	-1	1	-1	1	1
77	1	-1	-1	1	1	-1	-1
78	1	-1	-1	1	1	-1	1

\*channel numbers refer to Fig. 3-5

see Table 4-1 for coded relationships

Note: Coded values determined by methods described in Reference (A-1).

Table A-1: Coded Set of Detailed TORC Cases Used to Generate Response Surface (con't.)

Case Number	Inlet Flow Factors				Enthalpy Rise Factor	Systematic Pitch	Systematic Clad G.D.
	Channel [ ]	Channel [ ]	Channel [ ]	Channel [ ]			
79	1	-1	-1	1	1	1	-1
80	1	-1	-1	1	1	1	1
81	1	-1	1	-1	-1	-1	-1
82	1	-1	1	-1	-1	-1	1
83	1	-1	1	-1	-1	1	-1
84	1	-1	1	-1	-1	1	1
85	1	-1	1	-1	1	-1	-1
86	1	-1	1	-1	1	-1	1
87	1	-1	1	-1	1	1	-1
88	1	-1	1	-1	1	1	1
89	1	-1	1	1	-1	-1	-1
90	1	-1	1	1	-1	-1	1
91	1	-1	1	1	-1	1	-1

\*channel numbers refer to Fig. 3-5

see Table 4-1 for coded relationships

Note: Coded values determined by method described in Reference (A-1).

Table A-1: Coded Set of Detailed TORC Cases Used to Generate Response Surface (cont.)

Case Number	Inlet Flow Factors				Enthalpy Rise Factor	Systematic Fitch	Systematic Clad O.D.
	Channel [ ]	Channel [ ]	Channel [ ]	Channel [ ]			
92	1	-1	1	1	-1	1	1
93	1	-1	1	1	1	-1	-1
94	1	-1	1	1	1	-1	1
95	1	-1	1	1	1	1	-1
96	1	-1	1	1	1	1	1
97	1	1	-1	-1	-1	-1	-1
98	1	1	-1	-1	-1	-1	1
99	1	1	-1	-1	-1	1	-1
100	1	1	-1	-1	-1	1	1
101	1	1	-1	1	1	-1	-1
102	1	1	-1	1	1	-1	1
103	1	1	-1	1	1	1	-1
104	1	1	-1	1	1	1	1

channel numbers refer to Fig. 3-5

see Table 4-1 for coded relationships

Note: Coded values determined by method described in Reference (A-1).

Table A-1: Coded Set of Detailed TORC Cases Used to Generate Response Surface (con't.)

Case Number	Inlet Flow Factors				Enthalpy Rise Factor	Systematic Pitch	Systematic Clad G.D.
	Channel [ ]	Channel [ ]	Channel [ ]	Channel [ ]			
105	1	1	-1	1	-1	-1	-1
106	1	1	-1	1	-1	-1	1
107	1	1	-1	1	-1	1	-1
108	1	1	-1	1	-1	1	1
109	1	1	-1	1	1	-1	-1
110	1	1	-1	1	1	-1	1
111	1	1	-1	1	1	1	-1
112	1	1	-1	1	1	1	1
113	1	1	1	-1	-1	-1	-1
114	1	1	1	-1	-1	-1	1
115	1	1	1	-1	-1	1	-1
116	1	1	1	-1	-1	1	1
117	1	1	1	-1	1	-1	-1

\*channel numbers refer to Fig. 3-5

see Table 4-1 for coded relationships

Note: Coded values determined by method described in Reference (A-1).

Table A-1: Coded Set of Detailed TORC Cases Used to Generate Response Surface (con't.)

Case Number	Inlet Flow Factors				Inlet Velocity	Systematic Pitch	Systematic Clad O.S.
	Channel [ ]	Channel [ ]	Channel [ ]	Channel [ ]			
118	1	1	1	-1	1	-1	1
119	1	1	1	-1	1	1	-1
120	1	1	1	-1	1	1	1
121	1	1	1	1	-1	-1	-1
122	1	1	1	1	-1	-1	1
123	1	1	1	1	-1	1	-1
124	1	1	1	1	-1	1	1
125	1	1	1	1	1	-1	-1
126	1	1	1	1	1	-1	1
127	1	1	1	1	1	1	-1
128	1	1	1	1	1	1	1
129	0	0	0	0	0	0	0
130	1.91	0	0	0	0	0	0

\*channel numbers refer to Fig. 3-5

see Table 4-1 for coded relationships

Note: Coded values determined by method described in Reference (A-1).

Table A-1: Coded Set of Detailed TORC Cases Used to Generate Response Surface (con't.)



Case Number	Inlet Flow Factors		Initial Rise Factor	systematic Flad 0.0.
	Channel	Channel		
131	-1.91	0	0	0
132	0	1.91	0	0
133	0	-1.91	0	0
134	0	0	1.91	0
135	0	0	-1.91	0
136	0	0	0	0
137	0	0	1.91	0
138	0	0	-1.91	0
139	0	0	0	0
140	0	0	1.91	0
141	0	0	-1.91	0
142	0	0	0	1.91
143	0	0	0	-1.91

\*channel numbers refer to Fig. 3-5 see Table 4-1 for coded relationships

Note: Coded values determined by method described in Reference (A-1).

Table A-1: Coded Set of Detailed 1066 Gas is Used to Generate Response Surface (cont.)

Case Number	Inlet Flow Factor				Enthalpy Rise Factor	Systematic Pitch**	Systematic Clad O.D.**	Detailed TORC HRRR	Response TORC HRRR	Residual
	Channel	Channel	Channel	Channel						
1					.9882	.5763			.000	
2					.9882	.5763			.004	
3					.9882	.5788			-.003	
4					.9882	.5788			-.002	
5					1.012	.5763			.000	
6					1.012	.5763			.004	
7					1.012	.5788			-.002	
8					1.012	.5788			-.002	
9					.9882	.5763			.000	
10					.9882	.5763			.004	
11					.9882	.5788			-.003	
12					.9882	.5788			-.002	
13					1.012	.5763			.000	
14					1.012	.5763			.004	
15					1.012	.5788			-.002	

\*channel numbers refer to Fig. 3-5

\*\*all system parameters dimensionless except systematic pitch and clad O.D. (inches)

TABLE A-2: Comparison of TORC and Response Surface HRRR for Cases Used to Generate Response Surface

Case Number	Inlet Flow Factor				Enthalpy Rise Factor	Systematic Pitch**	Systematic Clad O.D.**	Detailed TORC RMSE	Response TORC RMSE	Residual*
	Channel	Channel	Channel	Channel						
16					1.0120	.5788				-.001
17					.9882	.5763				-.003
13					.9882	.5763				.000
19					.9882	.5788				.002
20					.9882	.5788				-.002
21					1.0120	.5763				-.003
22					1.0120	.5763				-.001
23					1.0120	.5788				.003
24					1.0120	.5788				-.001
25					.9882	.5763				-.001
26					.9882	.5763				-.002
27					.9882	.5788				.003
28					.9882	.5788				-.001
29					1.0120	.5763				-.002
30					1.0120	.5763				-.002

\*channel numbers refer to Fig. 3-5

\*\*all system parameters dimensionless except systematic pitch and clad O.D. (inches)

TABLE A-2: Comparison of TORC and Response Surface RMSE for Cases Used to Generate Response Surface (con't.)

Case Number	Inlet Flow Factor				Enthalpy Rise Factor	Systematic Pitch**	Systematic Clad O.D.**	Detailed TORC MUMDR	Response TORC MUMDR	Residual
	Channel	Channel	Channel	Channel						
31					1.0120	.5788				.003
32					1.0120	.5788				-.001
33					.9882	.5763				.000
34					.9882	.5763				.004
35					.9882	.5788				-.003
36					.9882	.5788				-.001
37					1.0120	.5763				.000
38					1.0120	.5763				.004
39					1.0120	.5788				-.002
40					1.0120	.5788				-.002
41					.9882	.5763				-.001
42					.9882	.5763				.004
43					.9882	.5788				-.002
44					.9882	.5788				-.002
45					1.0120	.5763				-.001

\*channel numbers refer to Fig. 3-5

\*\*all system parameters dimensionless except systematic pitch and clad O.D. (inches)

TABLE A-2: Comparison of TORC and Response Surface MUMDR for Cases Used to Generate Response Surface (con't.)

Case Number	Inlet Flow Factor				Enthalpy Rise Factor	Systematic Pitch**	Systematic Clad O.D.**	Detailed TORC NUMBER	Response TORC NUMBER	Residual
	Channel	Channel	Channel	Channel						
46					1.0120	.5763				.003
47					1.0120	.5788				-.002
48					1.0120	.5788				-.002
49					.9882	.5763				-.002
50					.9882	.5763				-.002
51					.9882	.5788				.003
52					.9882	.5788				-.002
53					1.0120	.5763				-.003
54					1.0120	.5763				-.002
55					1.0120	.5788				.003
56					1.0120	.5788				-.001
57					.9882	.5763				-.002
58					.9882	.5763				-.002
59					.9882	.5788				.004
60					.9882	.5788				.000

\*channel numbers refer to Fig. 3-5

\*\*all system parameters dimensionless except systematic pitch and clad O.D. (inches)

TABLE A-2: Comparison of TORC and Response Surface RPSBk for Cases Used to Generate Response Surface (con't)

Case Number	Inlet Flow Factor				Enthalpy Rise Factor	Systematic Pitch**	Systematic Clad O.D.**	Detailed TORC MINOR	Response TORC MINOR	Residual
	Channel	Channel	Channel	Channel						
61					1.0120	.5763			-.003	
62					1.0120	.5763			-.002	
63					1.0120	.5788			.003	
64					1.0120	.5788			-.001	
65					.9882	.5763			.002	
66					.9882	.5763			-.006	
67					.9882	.5788			.001	
68					.9882	.5788			.006	
69					1.0120	.5763			.002	
70					1.0120	.5763			-.006	
71					1.0120	.5788			.001	
72					1.0210	.5788			.002	
73					.9882	.5763			.003	
74					.9882	.5763			-.005	
75					.9822	.5788			.000	

\*Channel numbers refer to Fig. 3-5

\*\*All system parameters dimensionless except systematic pitch and clad O.D. (inches)

TABLE A-2: Comparison of TORC and Response Surface MINOR for Cases Used to Generate Response Surface (con't.)

Case Number	Inlet Flow Factor				Enthalpy Rise Factor	Systematic Pitch**	Systematic Clad O.D.**	Detailed TORC MINOR	Response TORC MINOR	Residual
	Channel	Channel	Channel	Channel						
76					.9882	.5788			.005	
77					1.0120	.5763			.003	
78					1.0120	.5763			-.005	
79					1.0120	.5788			.000	
80					1.0120	.5788			.004	
81					.9882	.5763			.001	
82					.9882	.5763			.003	
83					.9882	.5788			-.002	
84					.9882	.5788			-.002	
85					1.0120	.5763			.000	
86					1.0120	.5763			.003	
87					1.0120	.5788			-.001	
88					1.0120	.5788			-.001	
89					.9882	.5763			.000	
90					.9882	.5763			.003	

\*channel numbers refer to Fig. 3-5

\*\*all system parameters dimensionless except systematic pitch and clad O.D. (inches)

TABLE A-2: Comparison of TORC and Response Surface MINOR for Cases Used to Generate Response Surfaces (con't.)

Case No.	Inlet Flow Factor				Enthalpy Rise Factor	Systematic Pitch**	Systematic Clad O.D.**	Detailed TORC NUMBER	Response TORC NUMBER	Residual
	Channel 1	Channel 2	Channel 3	Channel 4						
91					.9882	.5788				-.002
92					.9882	.5788				-.002
93					1.0120	.5763				-.001
94					1.0120	.5763				.004
95					1.0120	.5788				-.002
96					1.0120	.5788				-.002
97					.9882	.5763				.003
98					.9882	.5763				-.005
99					.9882	.5788				.000
100					.9882	.5788				.005
101					1.0120	.5763				.003
102					1.0120	.5763				-.004
103					1.0120	.5788				-.001
104					1.0120	.5788				.004
105					.9882	.5763				.004

\*channel numbers refer to Fig. 3-5

\*\*all system parameters dimensionless except systematic pitch and clad O.D. (inches)

TABLE A-2: Comparison of TORC and Response Surface NUMBER for Cases Used to Generate Response Surface (con't.)



Case Number	Inlet Flow Factor				Enthalpy Rise Factor	Systematic Pitch**	Systematic Clad O.D.**	Detailed TORC MDNBR	Response TORC MDNBR	Residual
	Channel	Channel	Channel	Channel						
106					.9882	.5763			-.004	
107					.9882	.5788			-.002	
103					.9882	.5788			.004	
109					1.0120	.5763			.005	
110					1.0120	.5763			-.004	
111					1.0120	.5788			-.001	
112					1.0120	.5788			.003	
113					.9882	.5763			.000	
114					.9882	.5763			.004	
115					.9882	.5788			-.003	
116					.9882	.5788			-.002	
117					1.0120	.5763			-.001	
118					1.0120	.5763			.005	
119					1.0120	.5788			-.003	
120					1.0120	.5788			-.002	

\*Channel numbers refer to Fig. 3-5

\*\*All system parameters dimensionless except systematic pitch and clad O.D. (inches)

TABLE A-2: Comparison of TORC and Response Surface MDNBR for Cases Used to Generate Response Surface (con't.)

Case Number	Inlet Flow Factor				Enthalpy Rise Factor	Systematic Pitch**	Systematic Clad O.D.**	Detailed 10Kc MDR	Response 10Kc MDR	Residual
	Channel	Channel	Channel	Channel						
121					.9882	.5763				-.001
122					.9882	.5763				.005
123					.9882	.5788				-.002
124					.9882	.5788				-.002
125					1.0120	.5763				-.001
126					1.0120	.5763				.005
127					1.0120	.5788				-.002
128					1.0120	.5788				-.002
129					1.0000	.5776				-.002
130					1.0000	.5776				-.010
131					1.0000	.5776				.010
132					1.0000	.5776				.001
133					1.0000	.5776				-.001
134					1.0000	.5776				.007
135					1.0000	.5776				-.006

\* Channel numbers refer to Fig. 3-5

\*\*all system parameters dimensionless except systematic pitch and clad O.D. (inches)

TABLE A-2: Comparison of 10Kc and Response Surface MDR for Cases Used to Generate Response Surface (con't.)

Case Number	Inlet flow Factor				Enthalpy Rise Factor	Systematic Pitch**	Systematic Clad O.D.**	Detailed TORC M/NBR	Response TORC M/NBR	Residual
	Channel	Channel	Channel	Channel						
136	}	}	}	}	1.0000	.5776	}	}	}	-.001
137					1.0000	.5776				.001
138					1.0228	.5776				.001
139					.9774	.5776				.000
140					1.0000	.5799				.012
141					1.0000	.5752				-.011
142					1.0000	.5776				-.005
143					1.0000	.5776				.005

\*channel numbers refer to Fig. 3-5

\*\*all system parameters dimensionless except systematic pitch and clad O.D. (inches)

TABLE A-2: Comparison of TORC and Response Surface M/NBR for Cases Used to Generate Response Surface (con't.)